Chapter 23

Figure 23.1

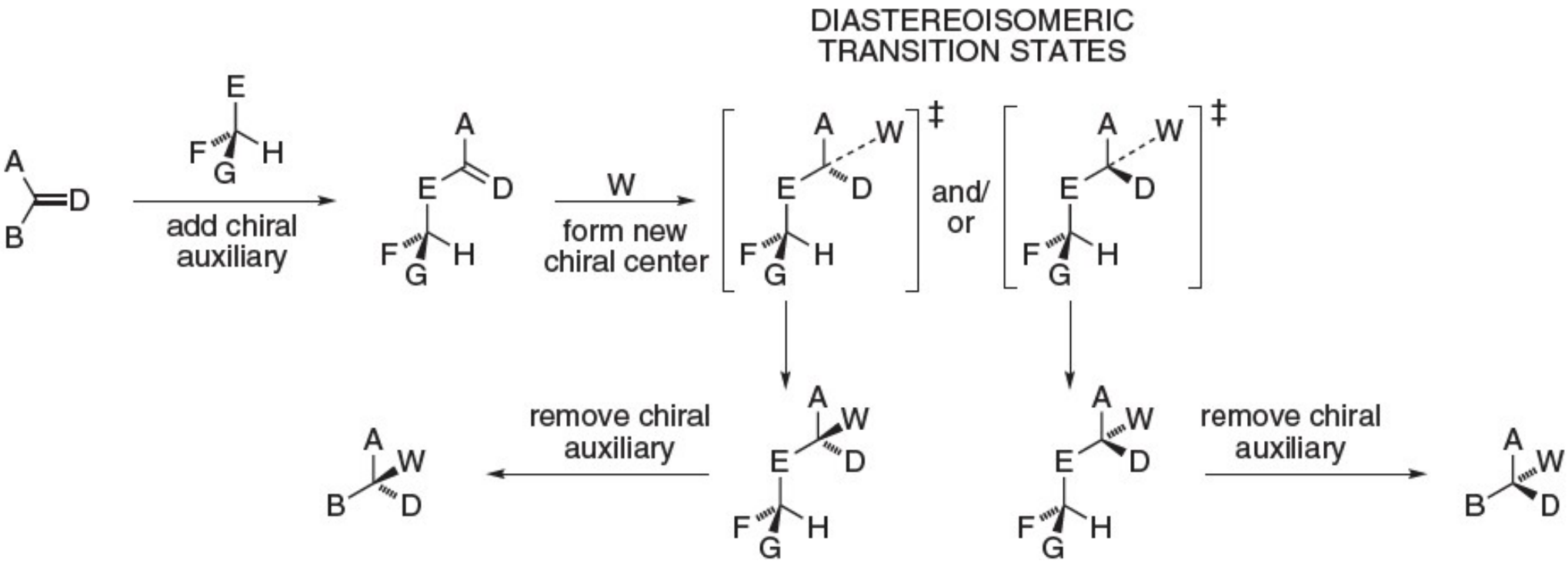

Formation of a chiral product enriched in one enantiomer by means of a chiral auxiliary.

Figure 23.2

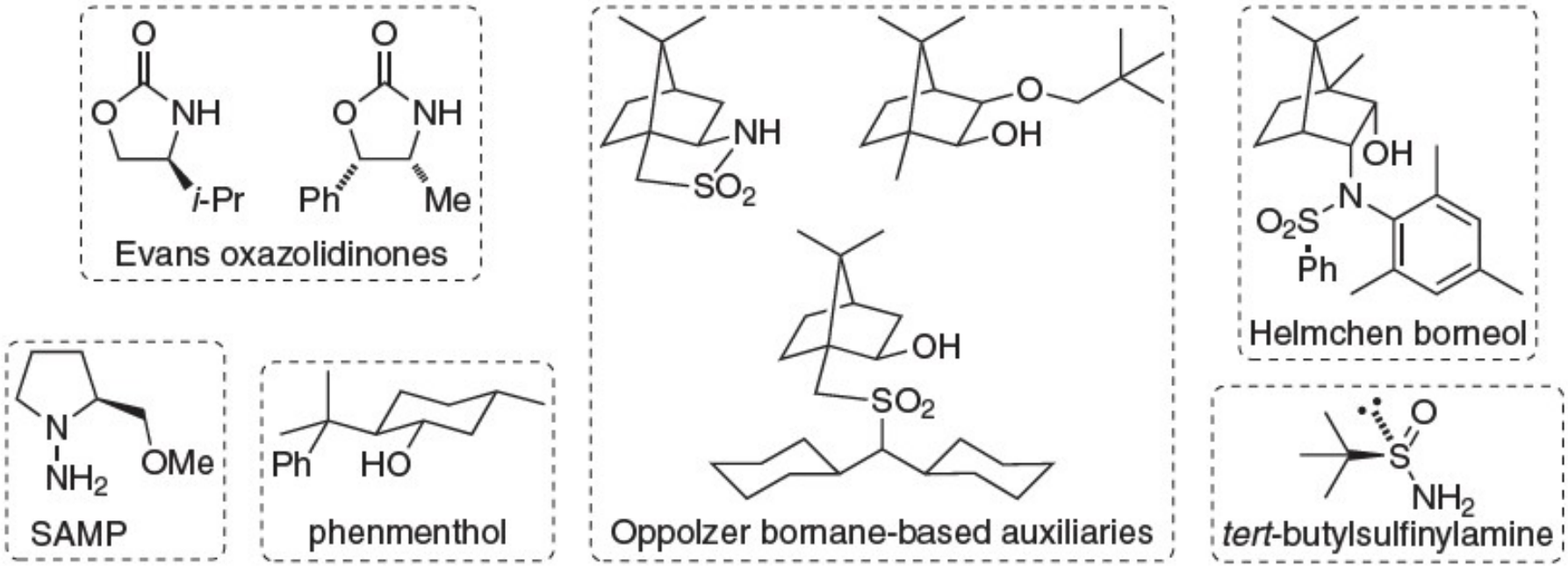

- Representative successful chiral auxiliaries

Figure 23.3

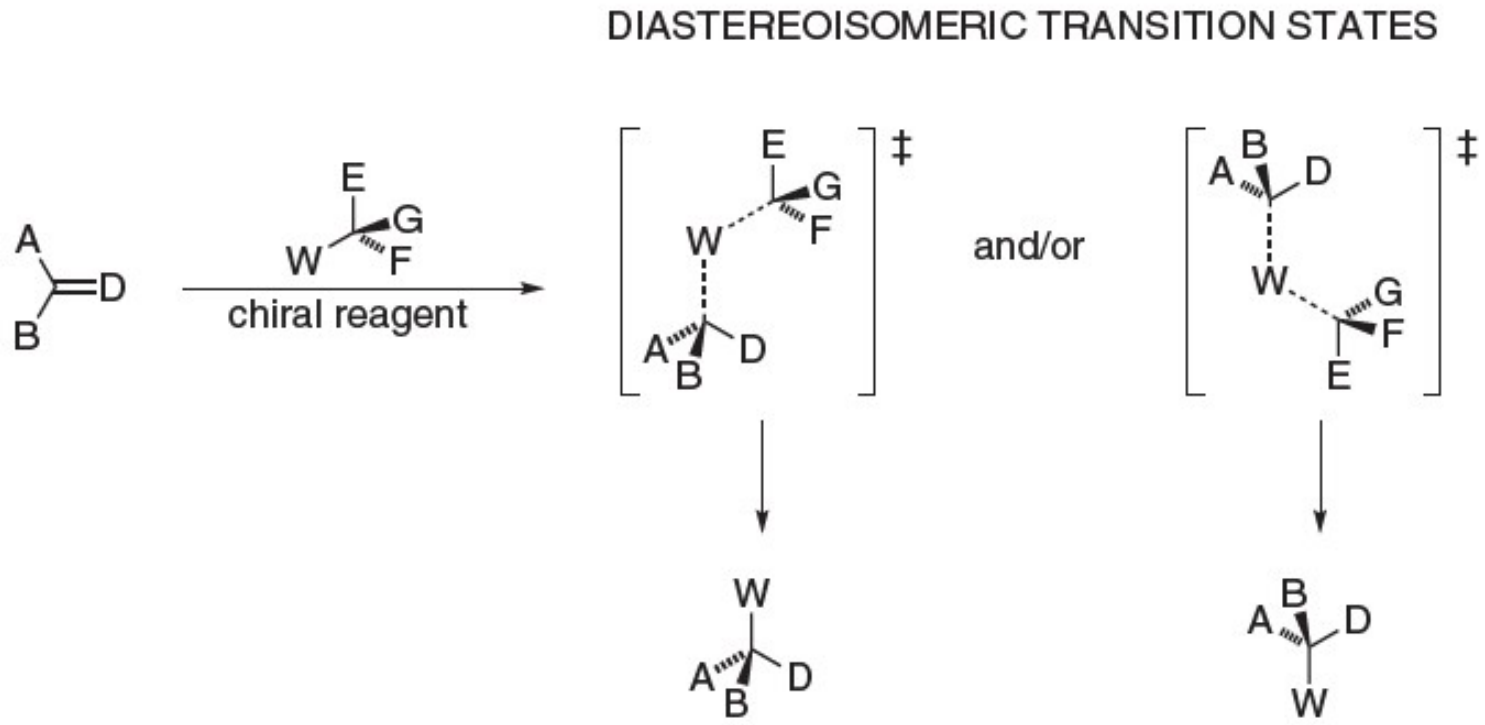

- Formation of a chiral product enriched in one enantiomer by means of a chiral reagent

Figure 23.4

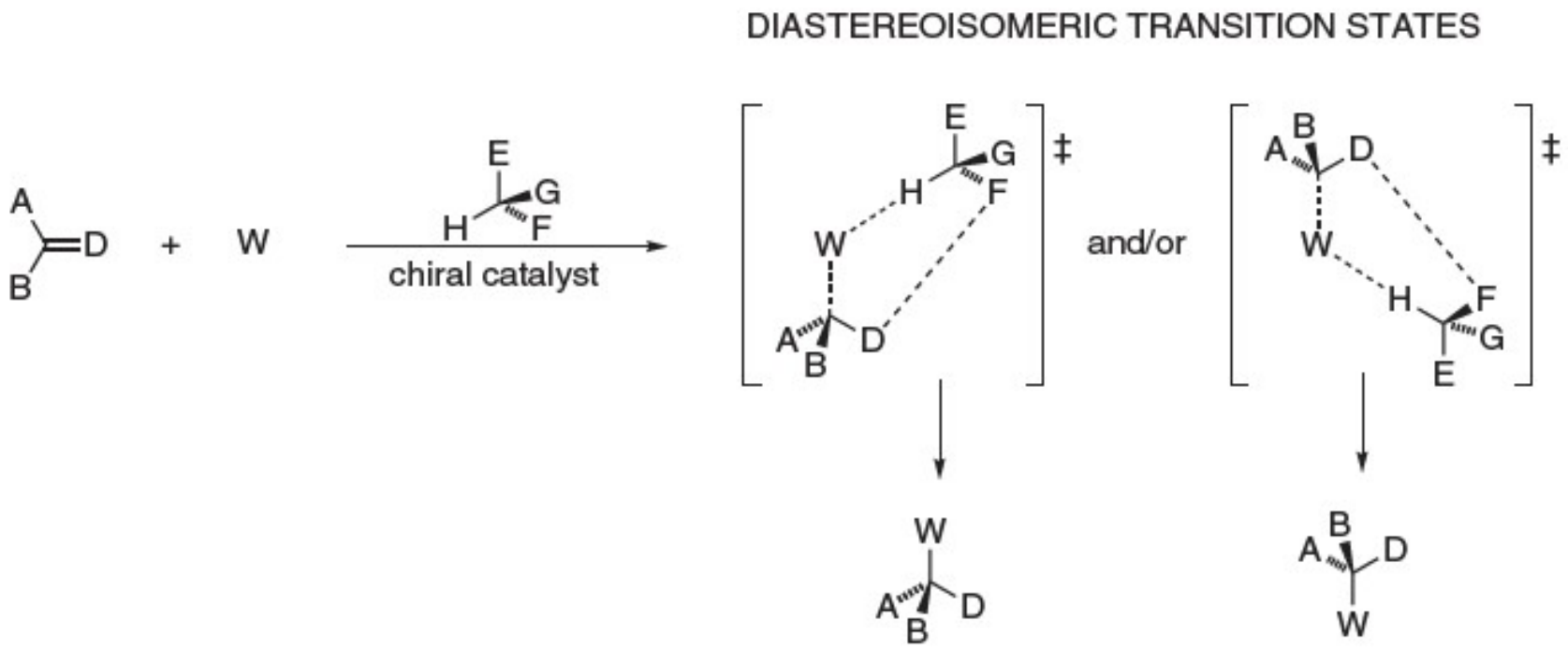

- Formation of a chiral product enriched in one enantiomer by means of a chiral catalyst

Figure 23.5

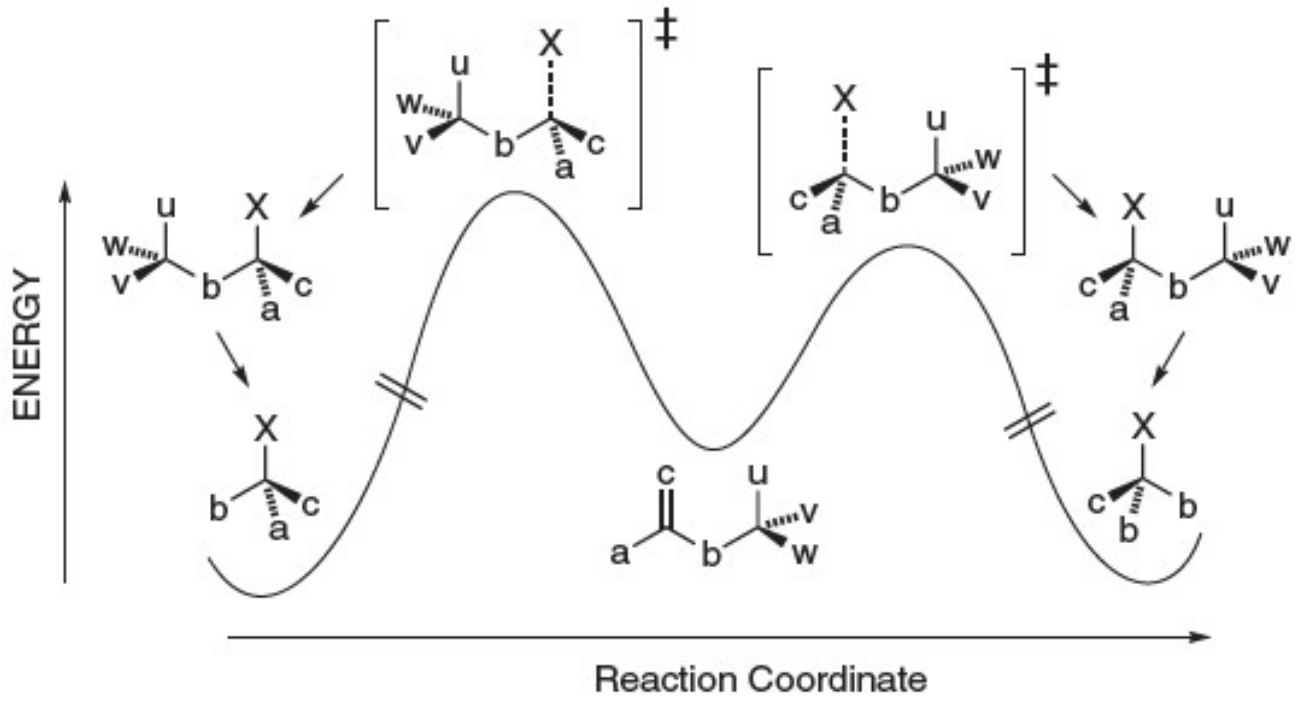

- Simple diastereoselection in a reaction between an achiral reactant and a prochiral substrate modified by a chiral auxiliary

Figure 23.6

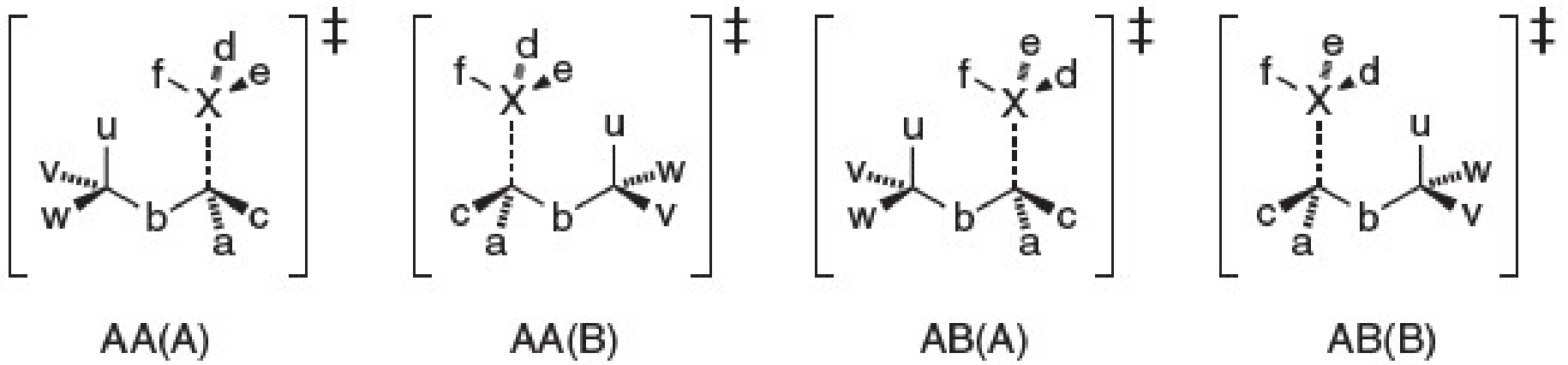

The four diastereomeric transition states for the reaction between two chiral molecules to generate a new chiral center

Figure 23.7

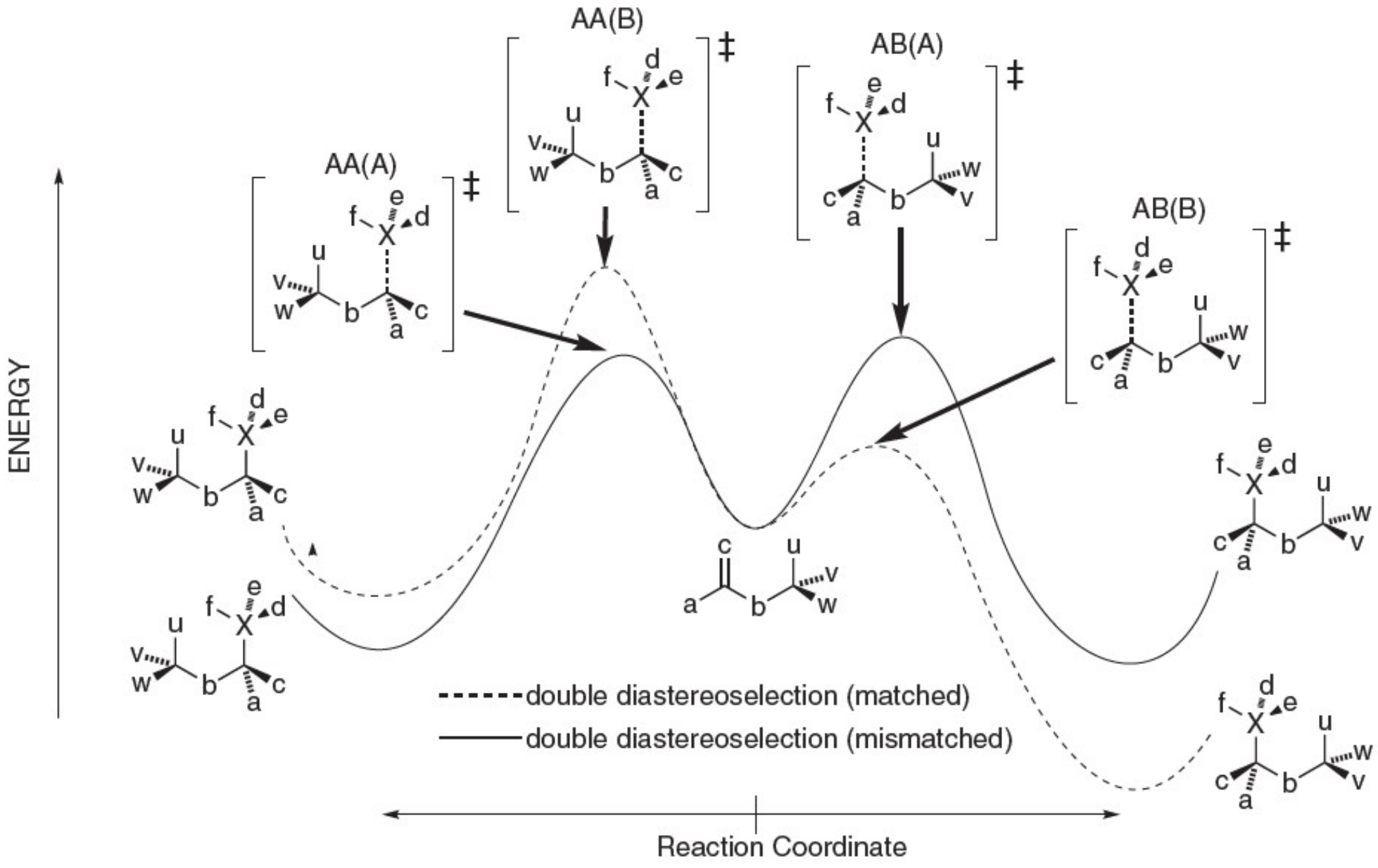
AA(B)
AB(A)
AA(A)
AB(B)
ENERGY
double diastereoselection (matched)
double diastereoselection (mismatched)
Reaction Coordinate

Figure 23.7

- The reaction energy profiles for the reaction between two chiral compounds to generate a new chiral center gives rise to four possible transition states, all of different energy. Based on this diagram, one would expect the product formed via AB(B) to dominate the product mixture, with a small amount of the product formed via AA(A), and negligible amounts of the other two diastereoisomers.

Figure 23.8

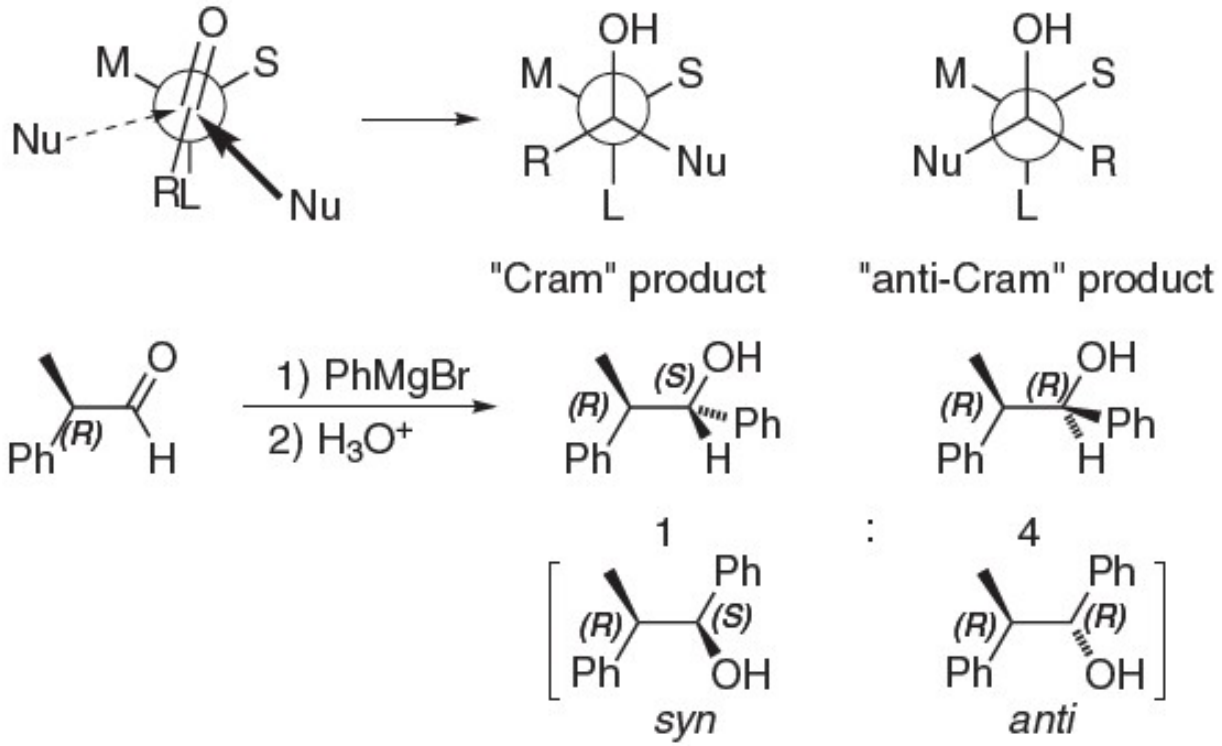

- Cram's Rule may be used to predict the stereochemistry of addition of nucleophiles to the carbonyl group of chiral aldehydes and ketones.

Figure 23.9

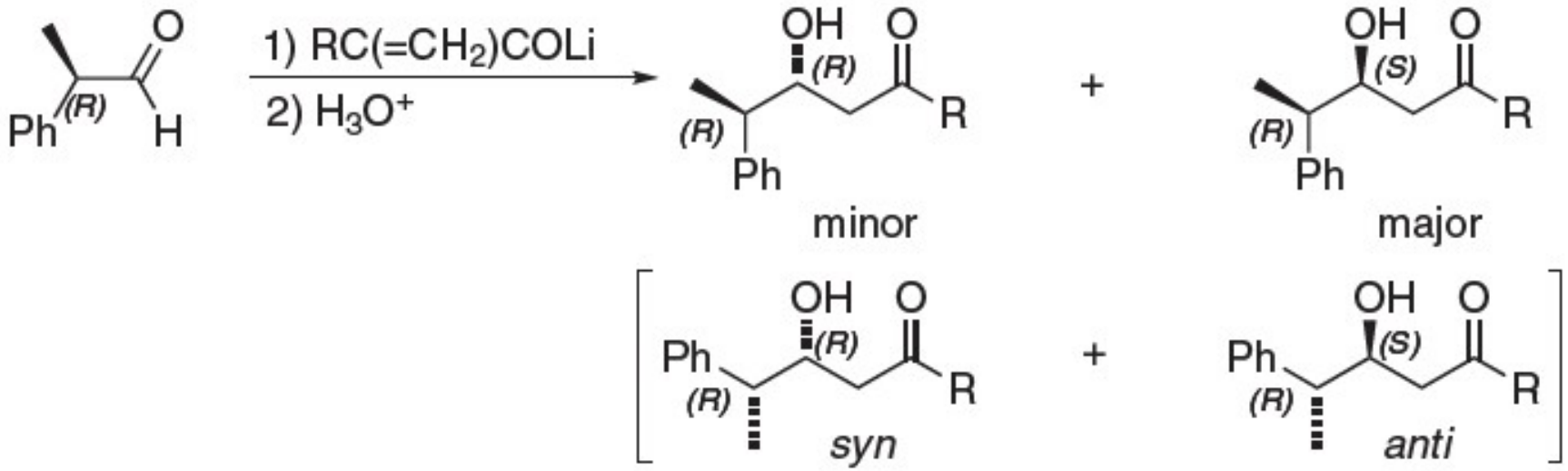

The kinetic aldol addition of the enolate of a chiral aldehyde to the enolate of an achiral methyl ketone gives the Cram (*anti*) isomer of the product as the major product

Stereochemistry in the aldol addition

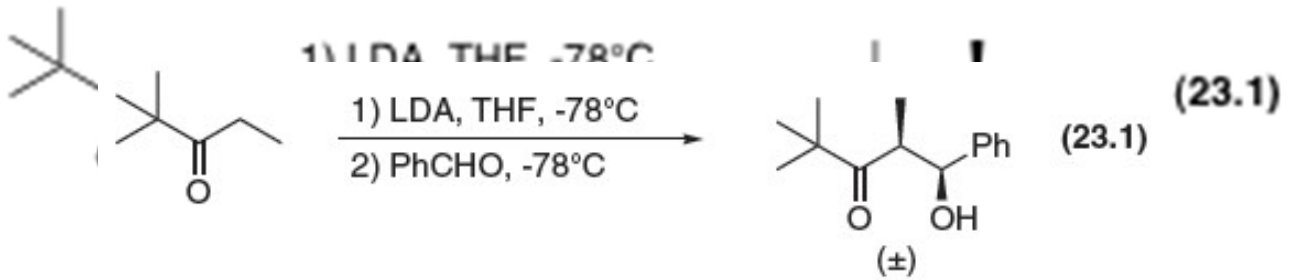

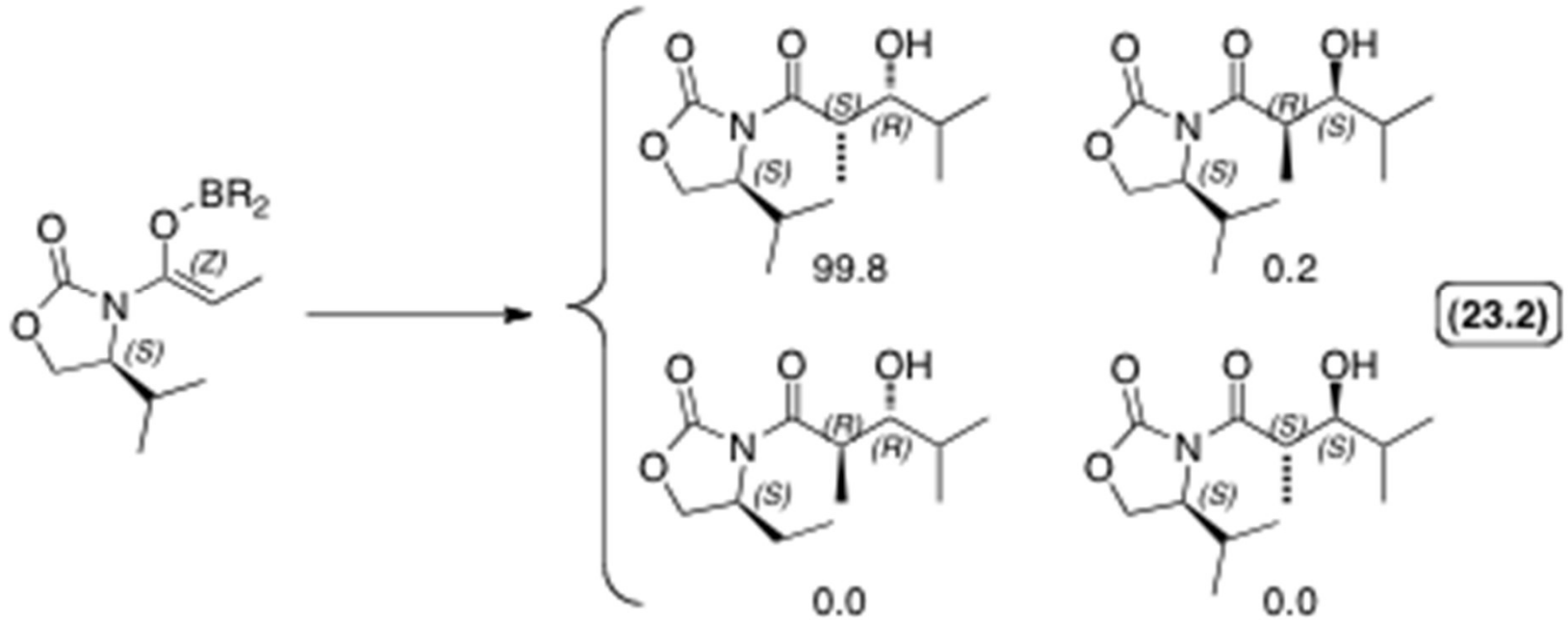

Figure 23.10

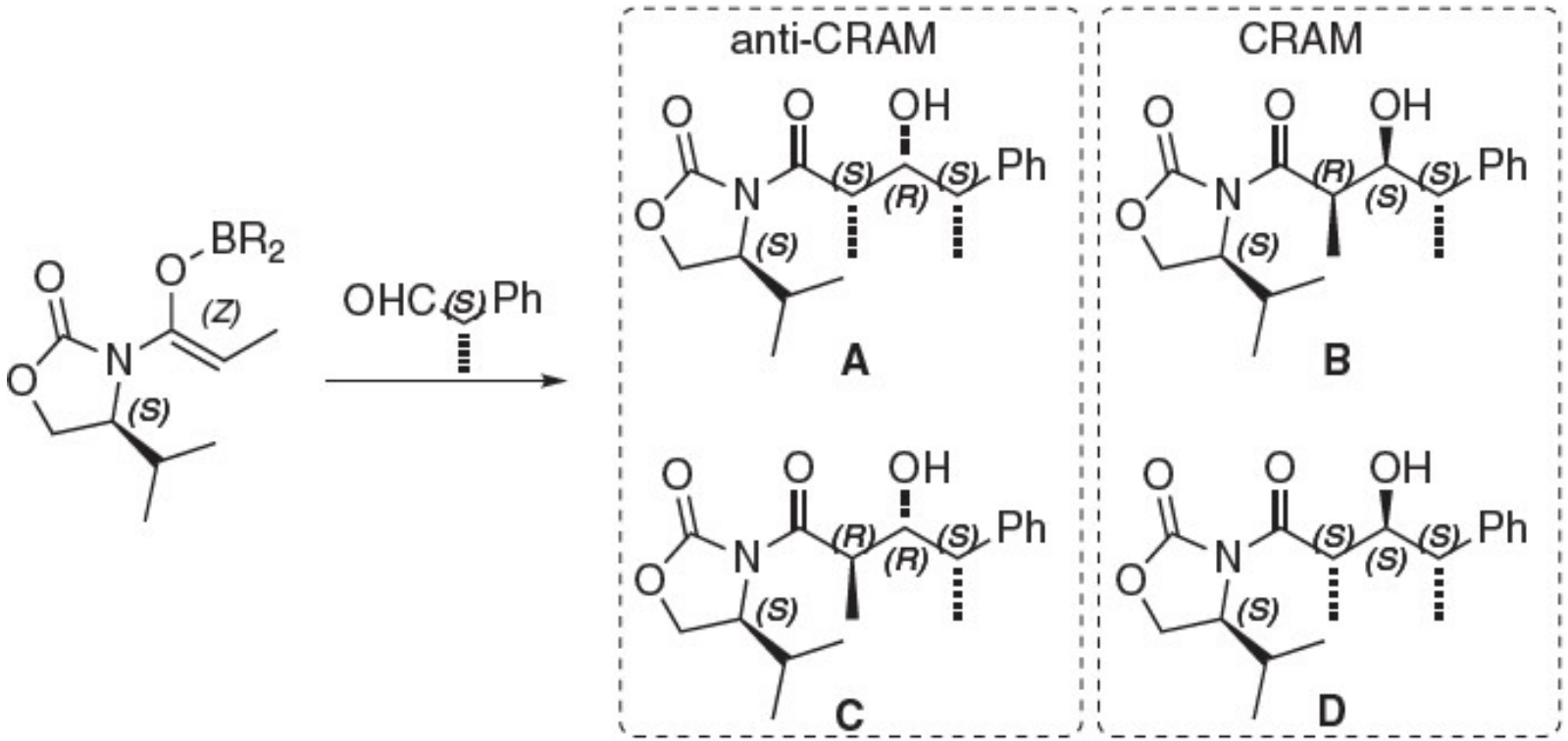

The possible diastereoisomeric products of the addition of the *S*-Evans chiral boron enolate to *S*-2-phenylpropanal

Figure 23.11

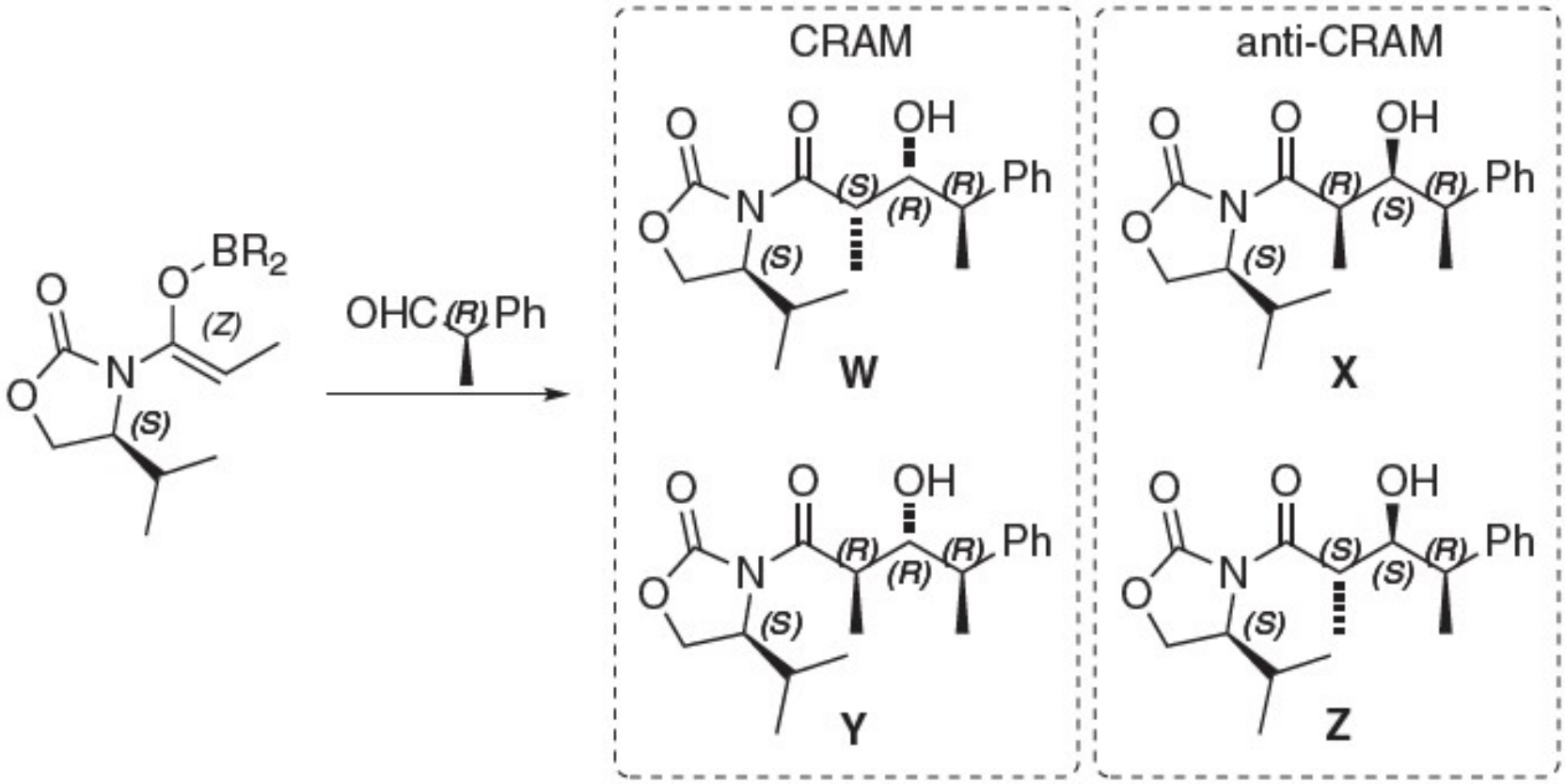

The possible diastereoisomeric products of the addition of the *S*-Evans chiral boron enolate to *R*-2-phenylpropanal

Figure 23.12

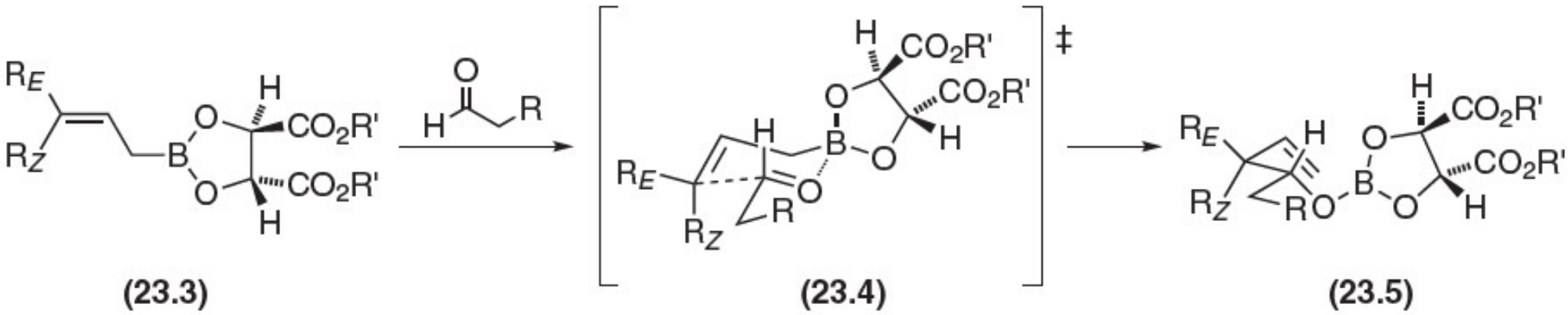

- Chiral crotylboration

Asymmetric crotylborations

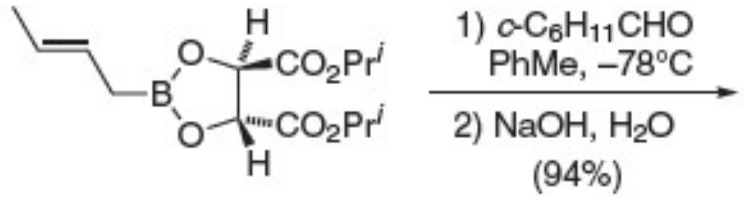

1) *c*-$C_6H_{11}CHO$, PhMe, –78°C
2) NaOH, H_2O
(94%)

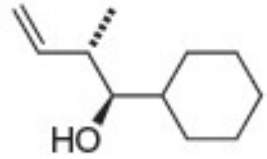

(23.6)

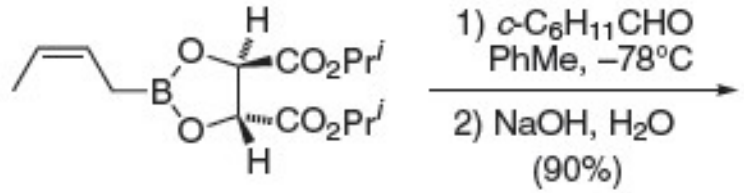

1) *c*-$C_6H_{11}CHO$, PhMe, –78°C
2) NaOH, H_2O
(90%)

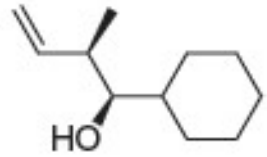

(23.7)

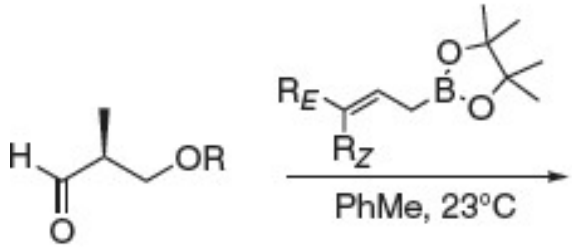

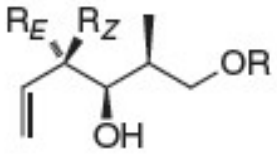

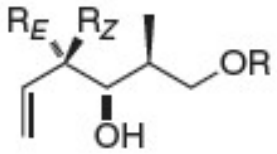

(23.8) **(23.9)** **(23.10)**

R = TBDMS; R_E= Me; R_Z = H	61	:	39
R = TBDPS; R_E= Me; R_Z = H	62	:	38
R = CH_2Ph; R_E= Me; R_Z = H	68	:	32
R = TBDMS; R_E= H; R_Z = Me	55	:	29
R = TBDPS; R_E= H; R_Z = Me	61	:	32
R = CH_2Ph; R_E= H; R_Z = Me	61	:	32

Asymmetric crotylborations: Matched and mismatched reagents

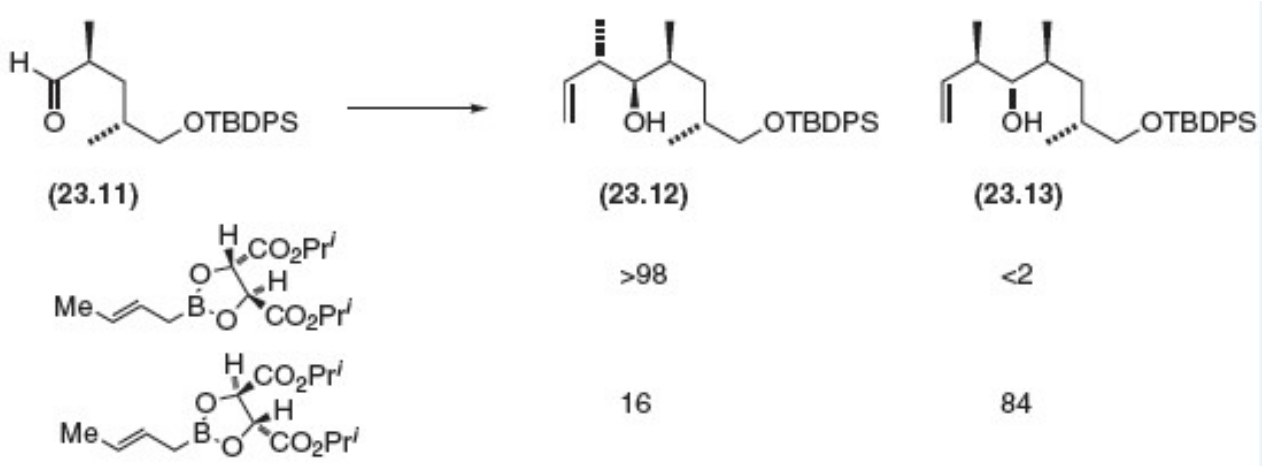

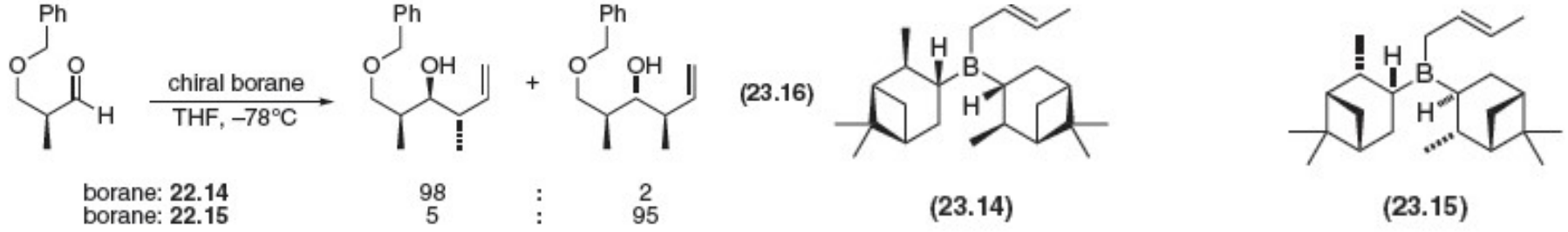

- The stereochemistry of the crotylborane fixes the stereochemistry of the product
- the Brown pinane-based boranes give higher e.e. in the mismatched reaction than the Roush crotylboronates
- reactions between matched reagents are in blue; mismatched results are in red

Figure 23.13

The possible stereochemical outcomes of asymmetric aldol addition reactions. In the Evans stereochemistry, the alkyl group *cis* to boron ends up *syn* to the directing group in the conformation drawn.

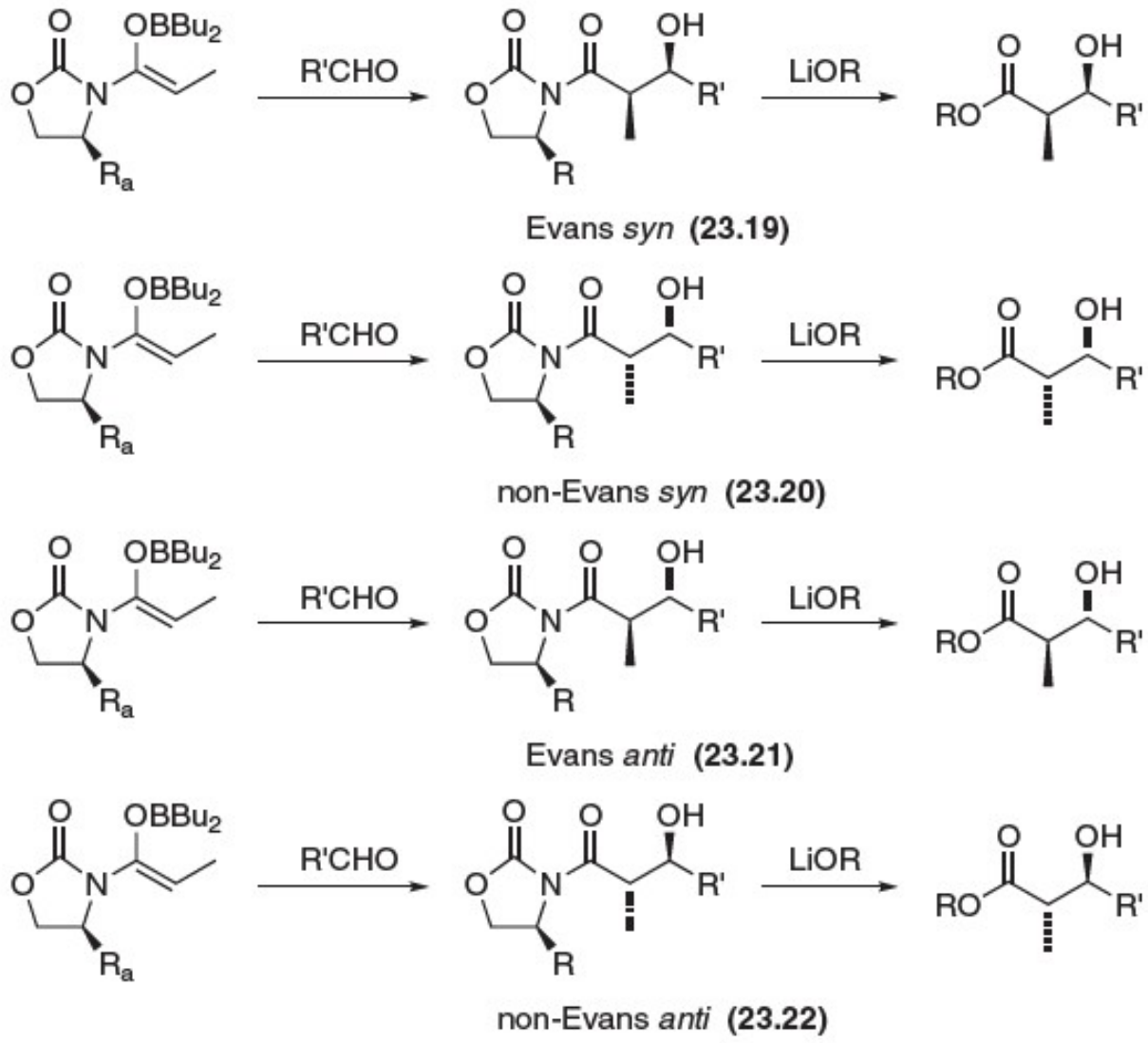

Figure 23.14

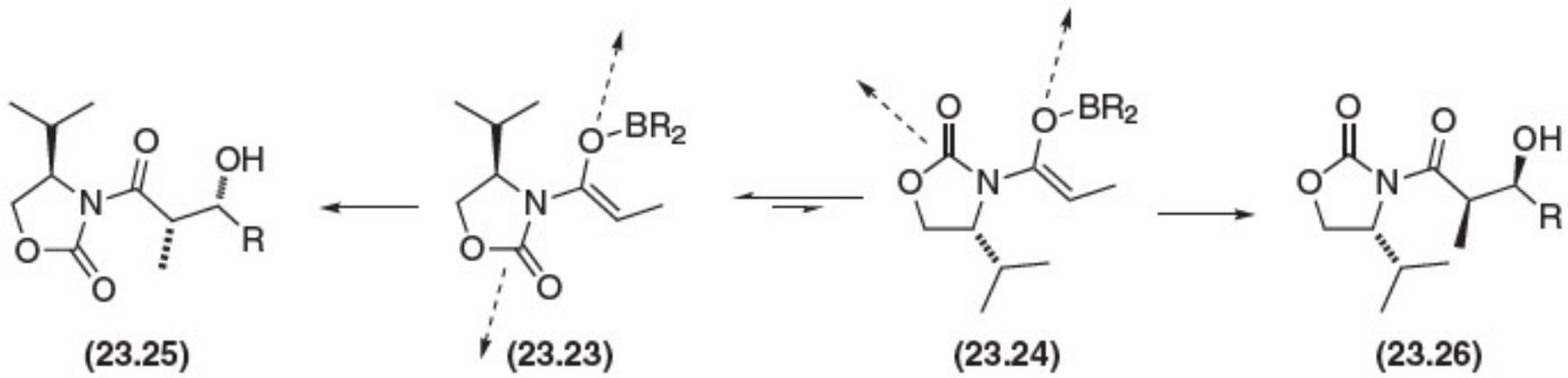

Rationalizing the stereochemistry of the Evans aldol addition of boron enolates

Figure 23.15

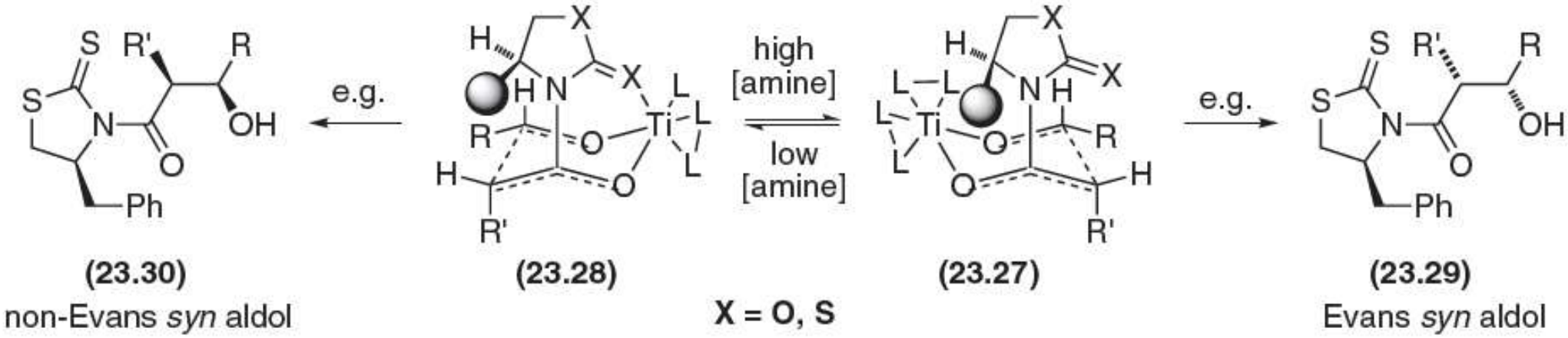

Stereochemical reversal by diamines in the aldol additions of titanium enolates

Chiral sulfinylamines and sulfinylimines

- this chiral auxiliary is relatively easily obtained as either enantiomer
- chirality is generated by the configurationally stable chiral sulfur
- deprotonation is effected with LDA; the resultant anion reacts with alkyl halides or with aldehydes
- the β-hydroxyalkylsulfinylimines formed in the reaction with aldehydes can be further elaborated to give stereochemically defined chiral β-hydroxyamines or chiral β-hydroxyketones
- the sulfinyl group is removed under mild conditions, and resembles the Boc group in this way

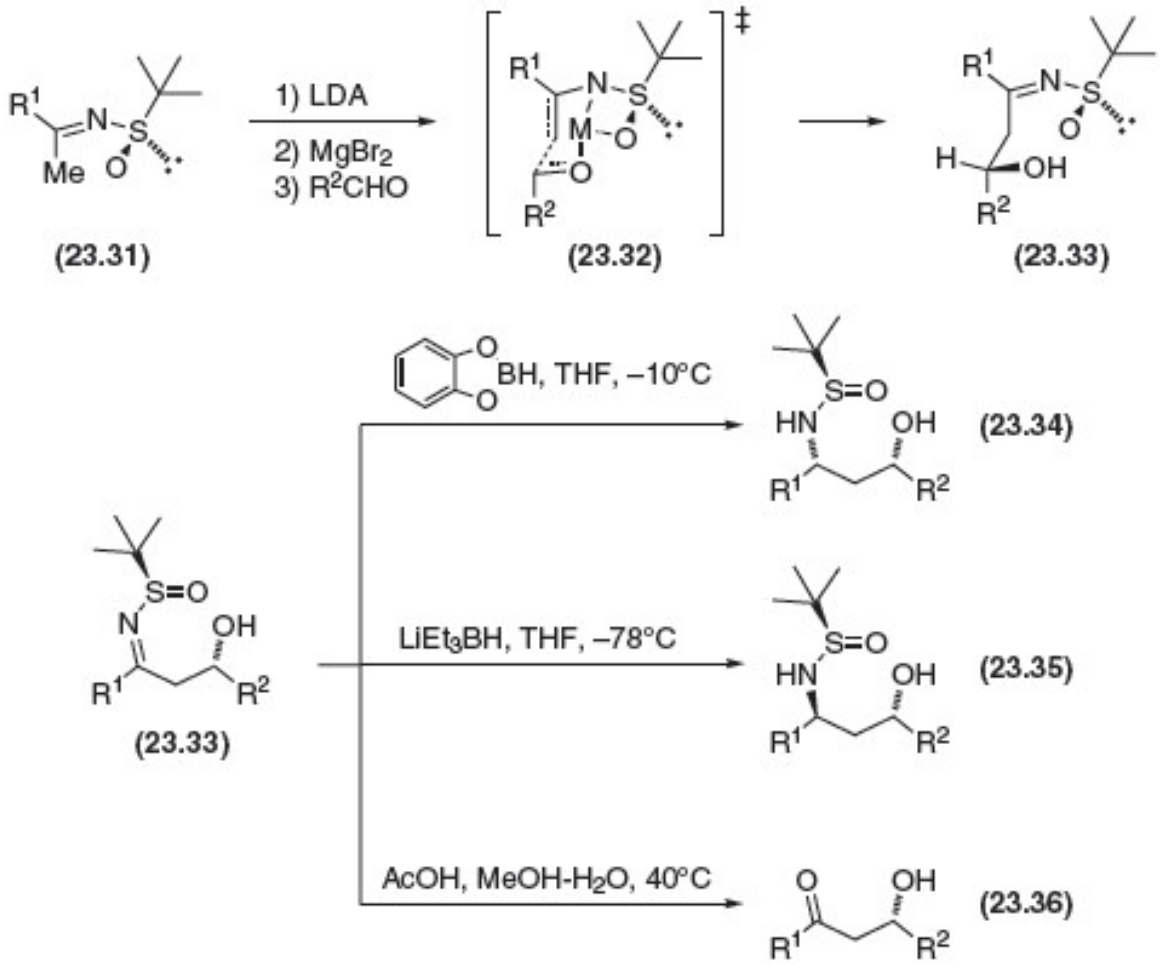

Phenmenthyl acrylates in the Diels-Alder reaction

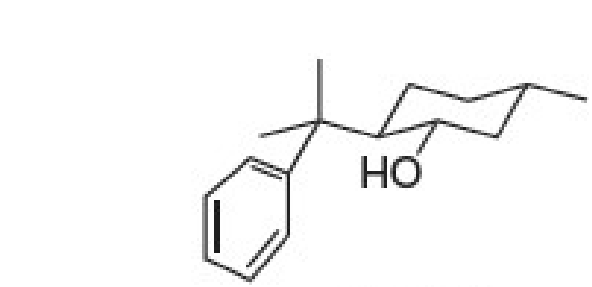

(23.37)

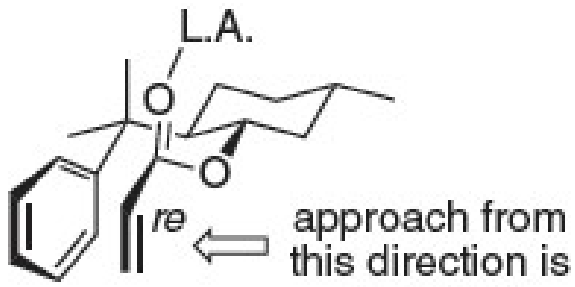

(23.38)

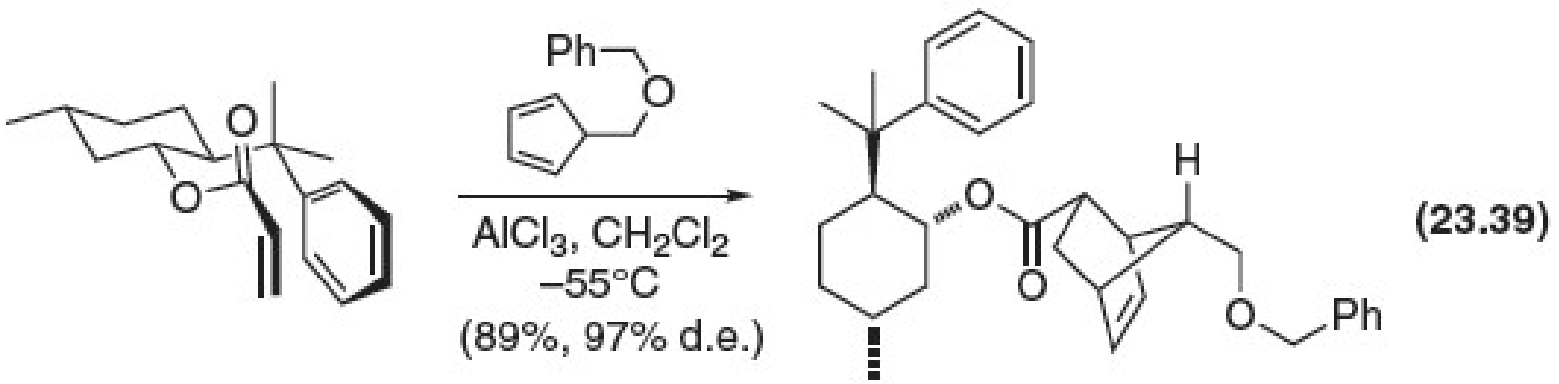

(23.39)

- diastereocontrol is effected by π stacking between the phenyl group and the acrylate π bond

Figure 23.16

Preparation of the 8-phenylmenthol auxiliary from pulegone

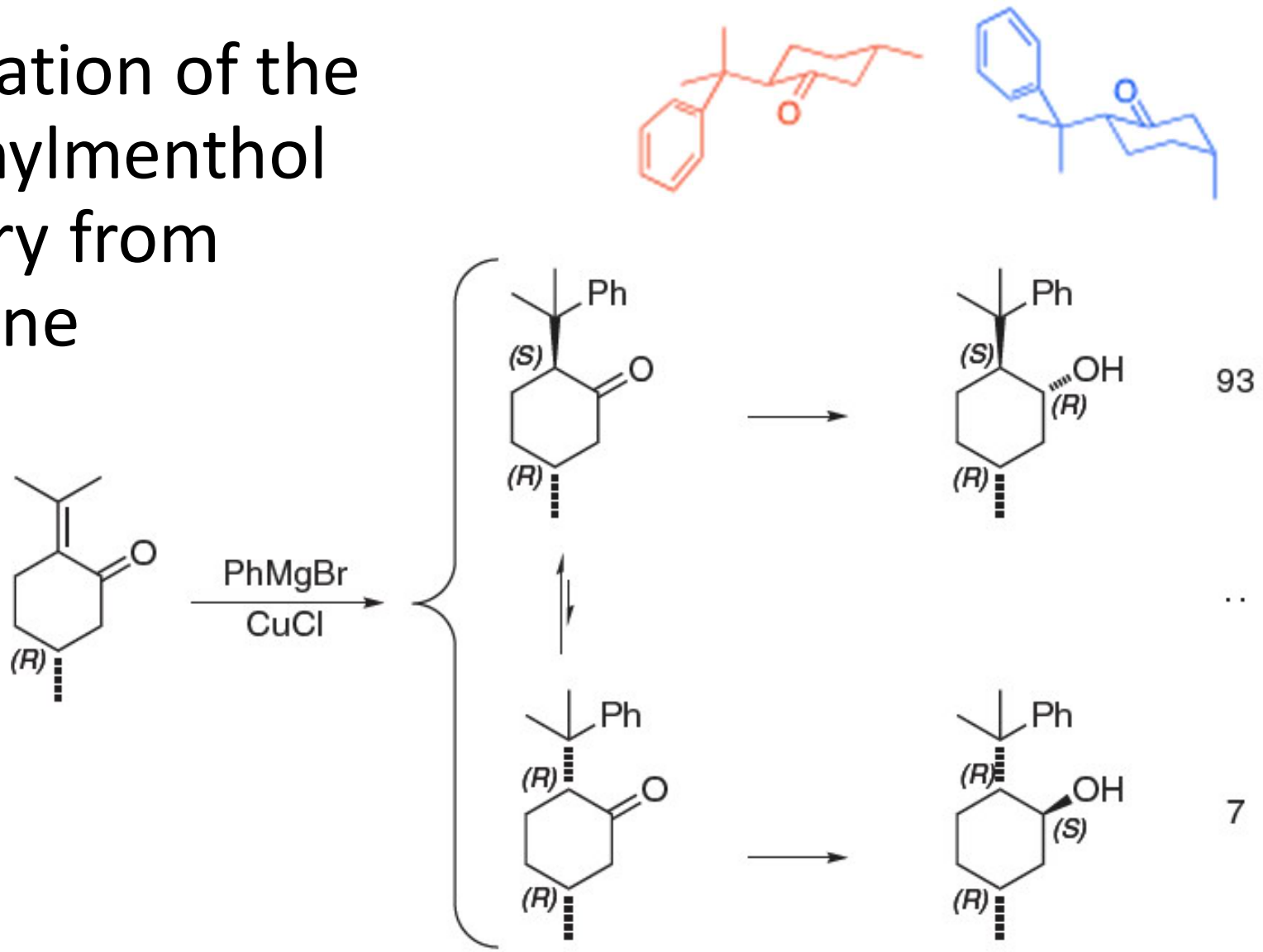

Figure 23.17

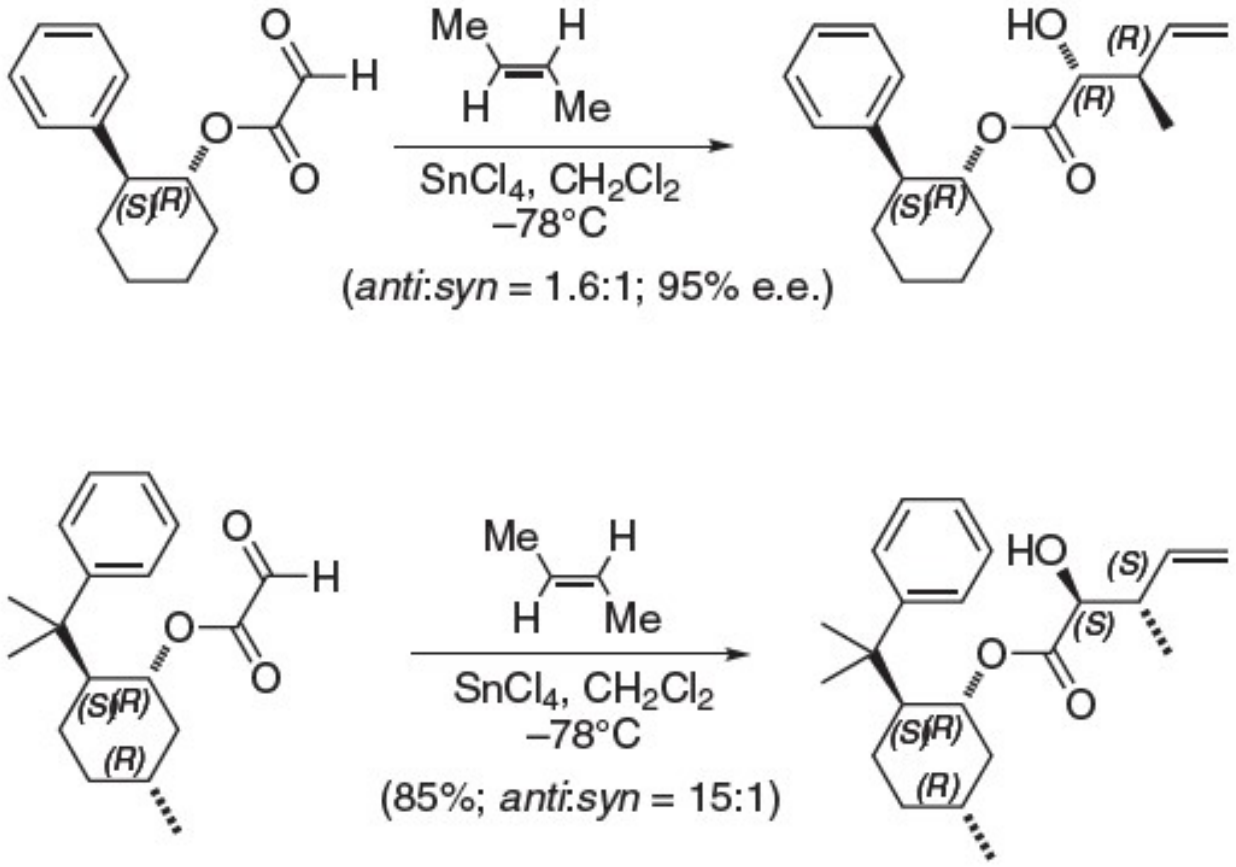

- Asymmetric ene reactions of glyoxylate esters

Oxazolidinone amides: asymmetric Diels-Alder reactions

Lewis acid complexes of the acrylamides of chiral oxazolidinones exhibit high enantioselectivity in Diels-Alder reactions

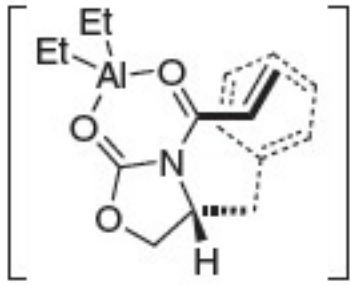

$\ominus$ Et_2AlCl_2 **(23.40)**

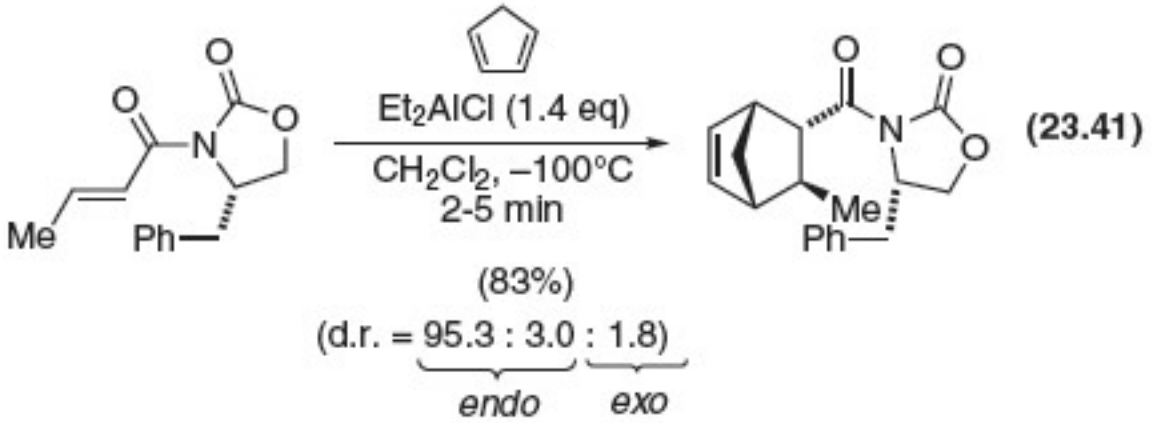

(23.41)

(83%)

(d.r. = 95.3 : 3.0 : 1.8)

endo *exo*

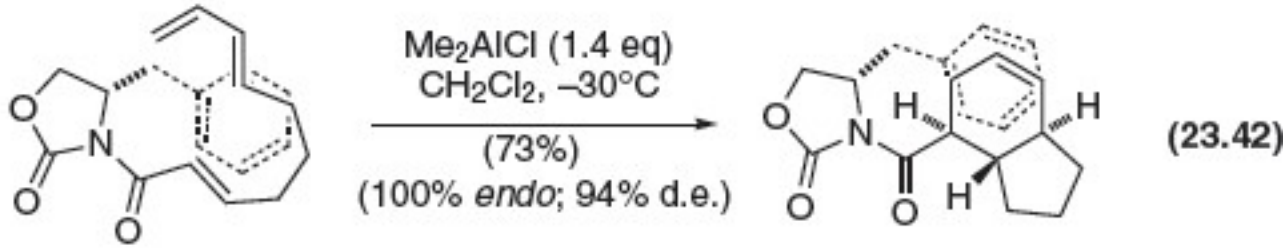

(23.42)

Oppolzer bornanes in Diels-Alder reactions

- both classes of chiral auxiliary give high levels of asymmetric induction

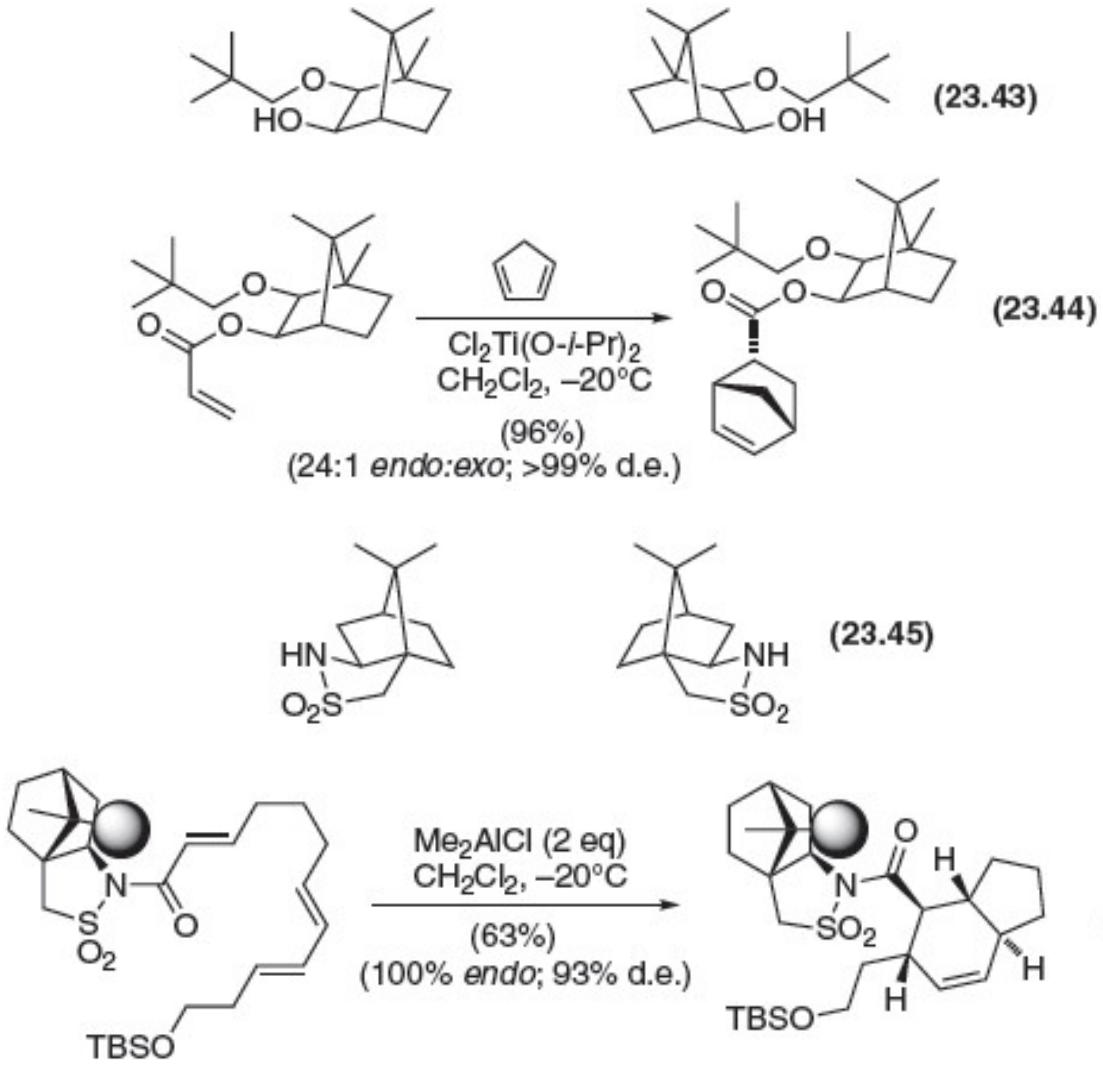

Nucleophilic addition to chiral sulfinylimines

- There is a very strong preference for the *s-cis* conformation of the sulfinylimine
  - in this conformation, there is the possibility of significant π delocalization of the lone pair on nitrogen into the S—O σ^* orbital.
- addition of the Grignard reagent occurs through a cyclic activated complex
- stereochemistry of the addition is reversed when alkyllithium reagents are used as the nucleophiles in the presence of Lewis acid additives, or a coordinating solvent
  - in this case, the reaction proceeds through an open transition state, making the addition intermolecular rather than intramolecular

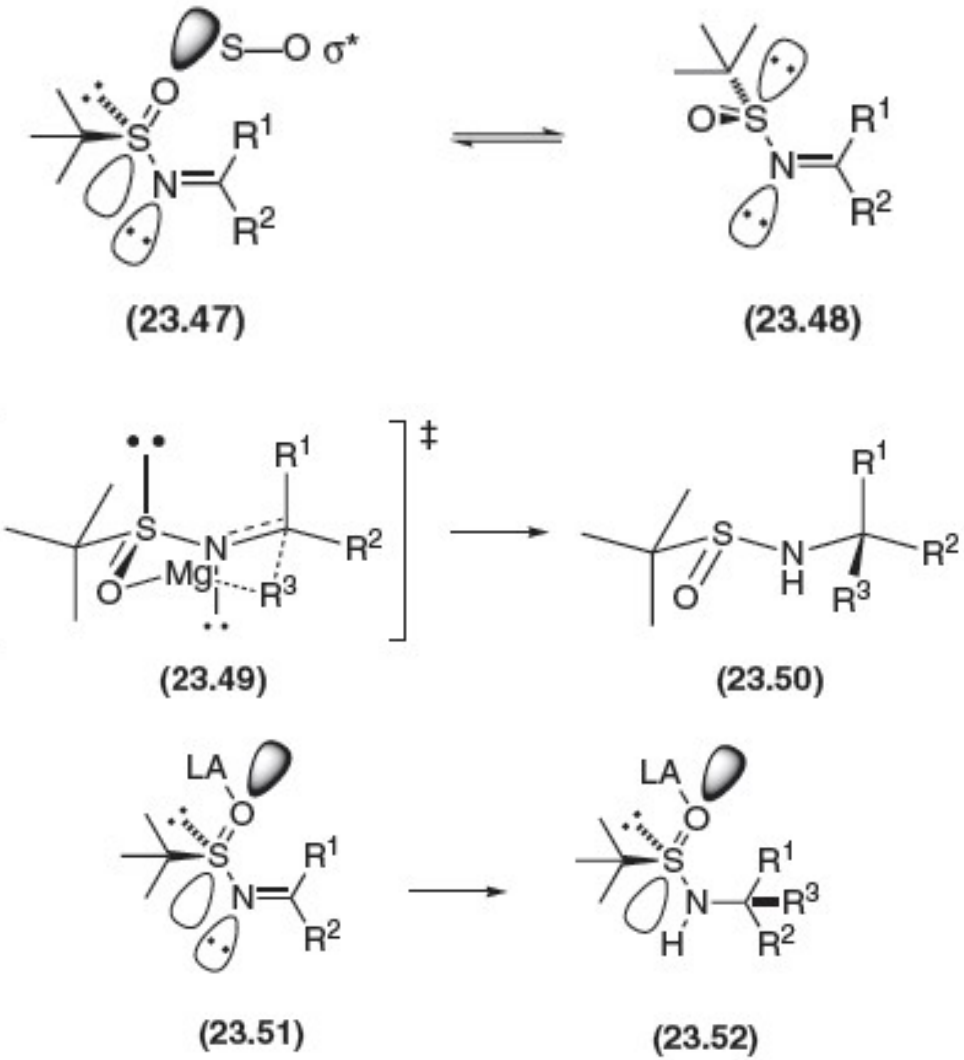

Representative Griognard additions to chiral sulfinylamines

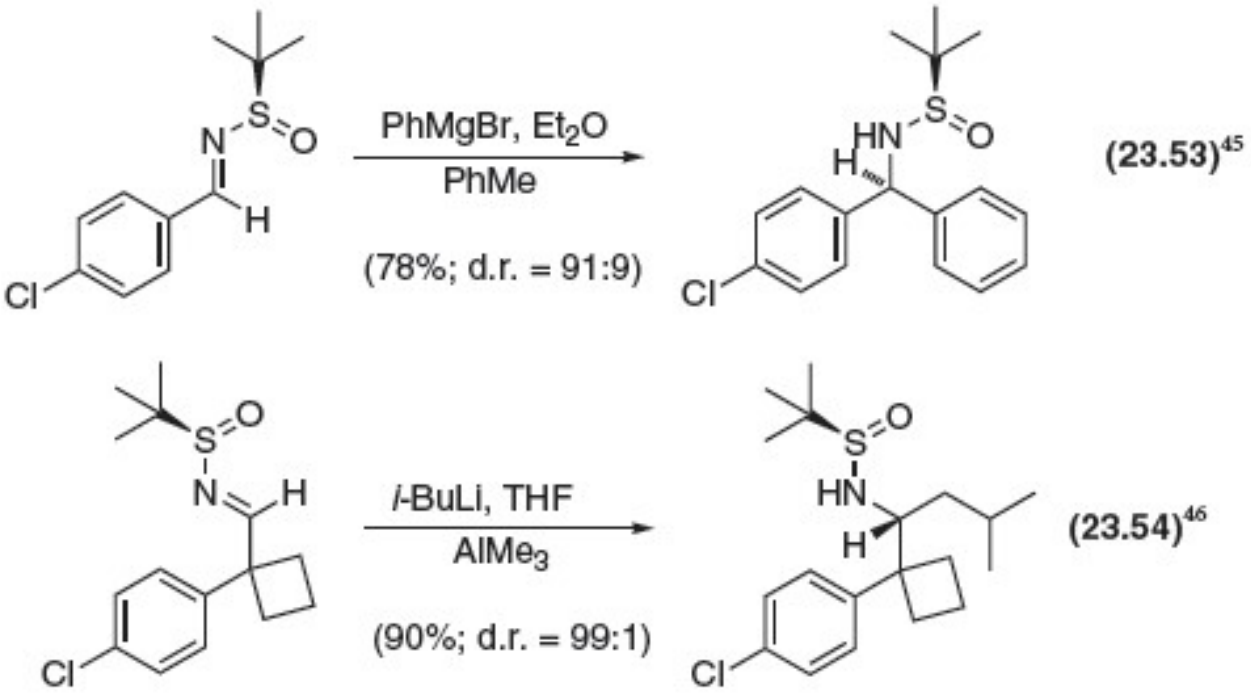

- Note how the stereochemistry of the addition is reversed when the Lewis acid, trimethylaluminum, is part of the reaction mixture

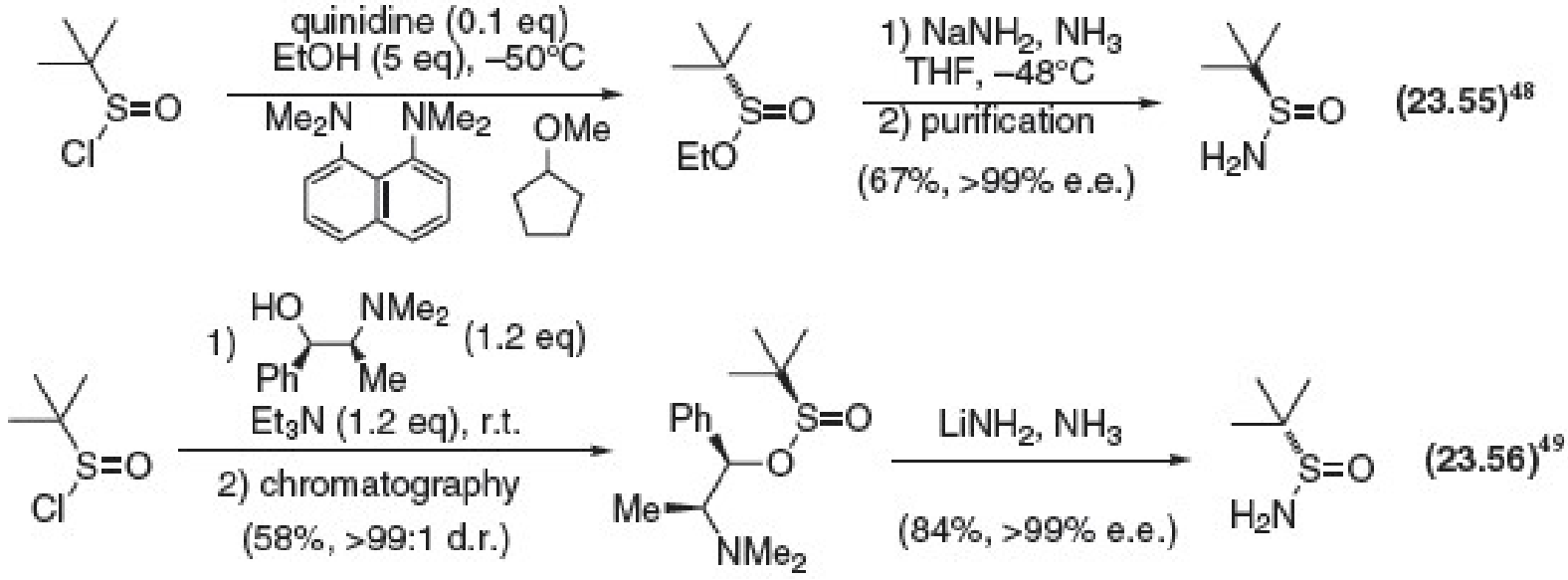

- the chiral sulfinylamine auxiliary can be made either by asymmetric synthesis of the sulfinate ester (which is configurationally stable) or by synthesis and chromatographic separation of the diastereoisomeric esters from the pseudoephedrine derivative

Representative asymmetric conjugate additions

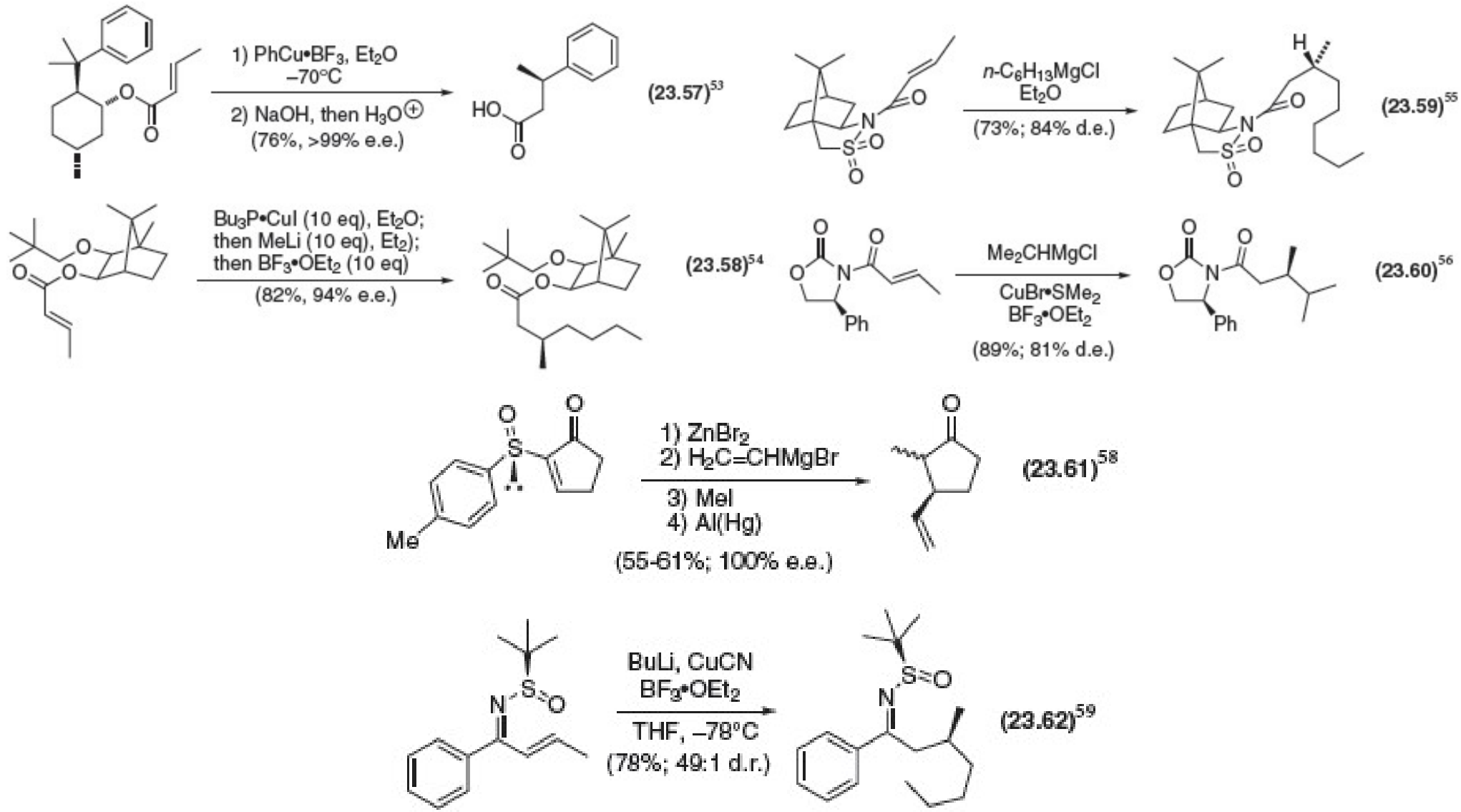

Asymmetric substitution at the α carbon

- there are two ways to accomplish this transformation
  - alkylation at the α carbon
  - oxidation at the α carbon
- thd choice of base can affect the regiochemistry of deprotonation and alkylation of cyclohexylimines

(23.63)

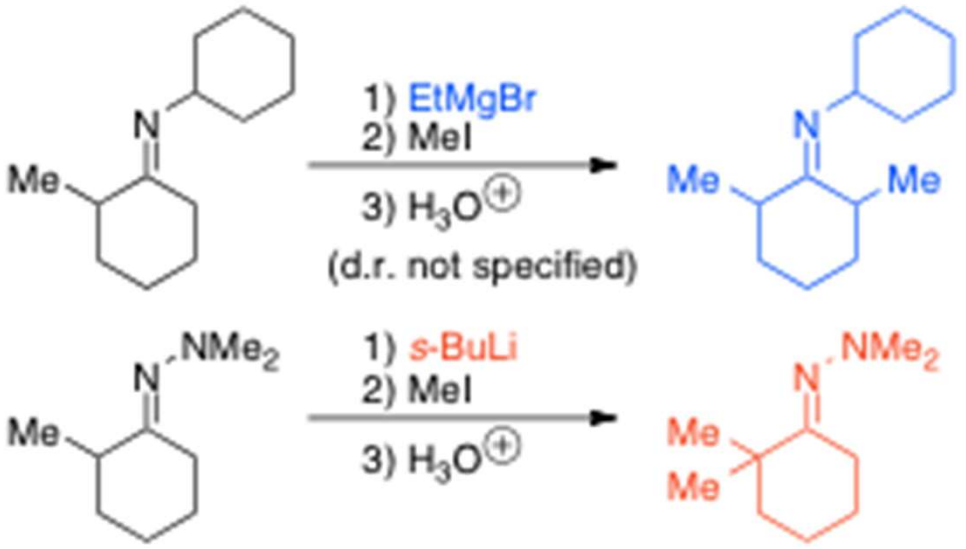

(23.64)

Alkylation of SAMP/RAMP hyrazones

- chiral auxiliaries for the alkylation of ketones and aldehydes
- deprotonation of the SAMP/RAMP hydrazones of acyclic ketones leads to the *E* double bond, and the eclipsed conformation of the C—N bond with nitrogen and carbon eclipsed
- quasi-1,3-diaxial interaction between the methylene group of the pyrrolidine ring and the approaching alkyl halide hinders the approach to one face of enolate

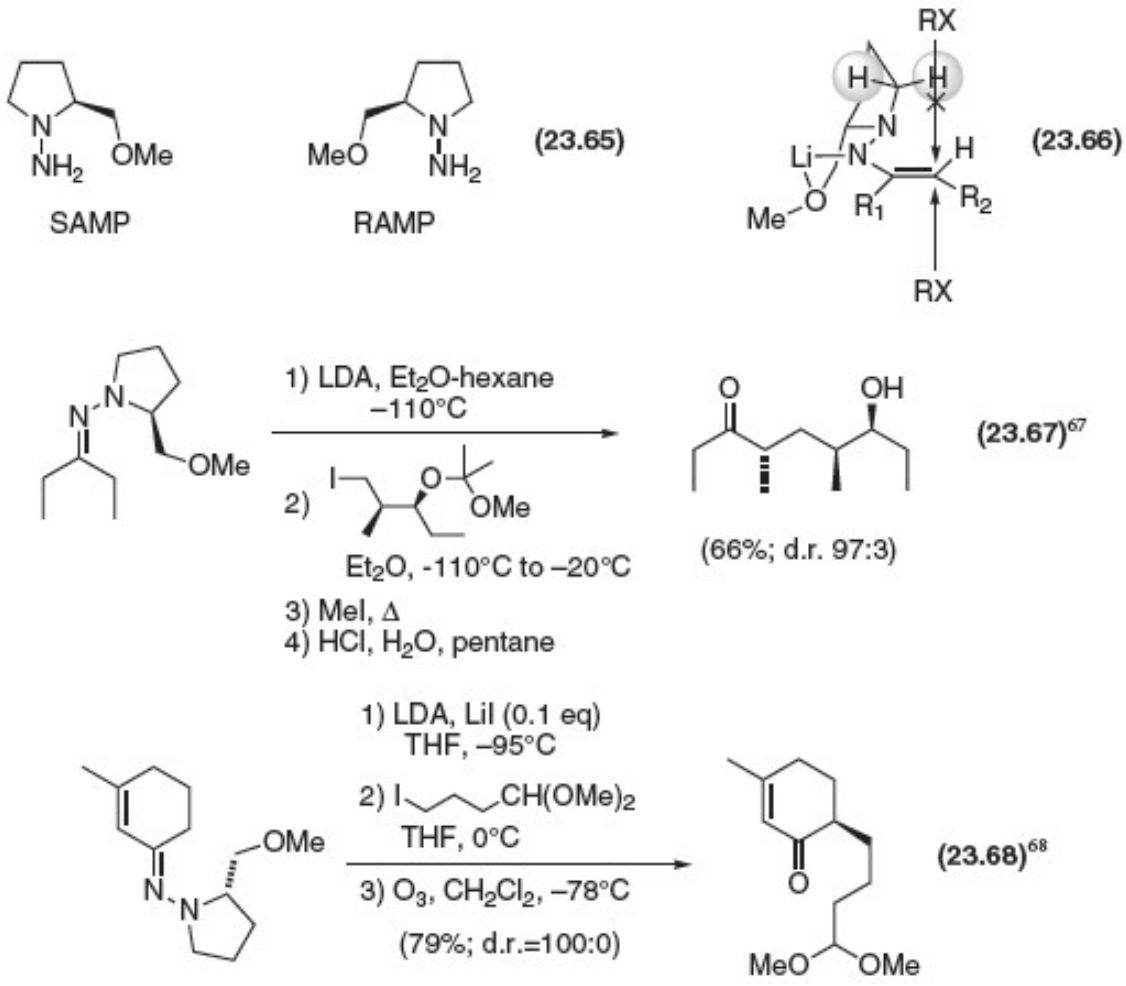

Figure 23.18

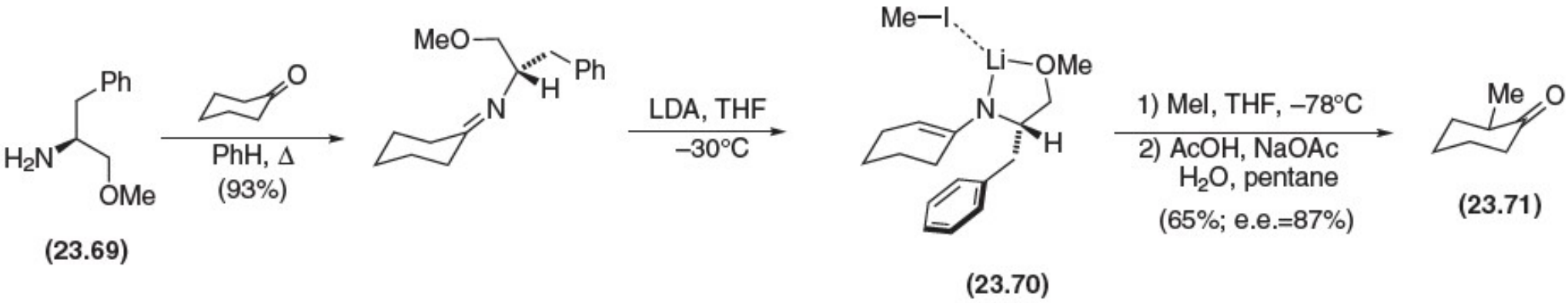

- Alkylation of chiral imines

Alkylation of chiral oxazolines

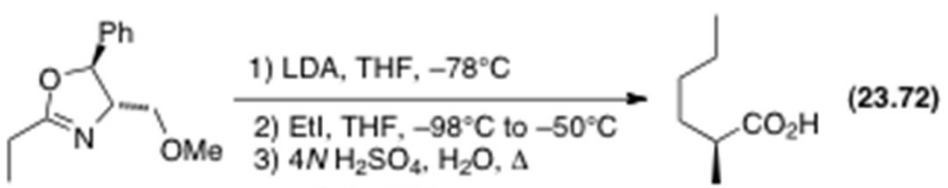

(23.72)

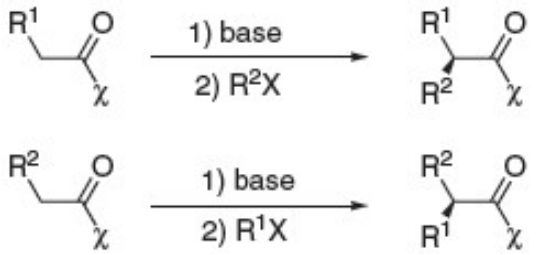

(23.73)

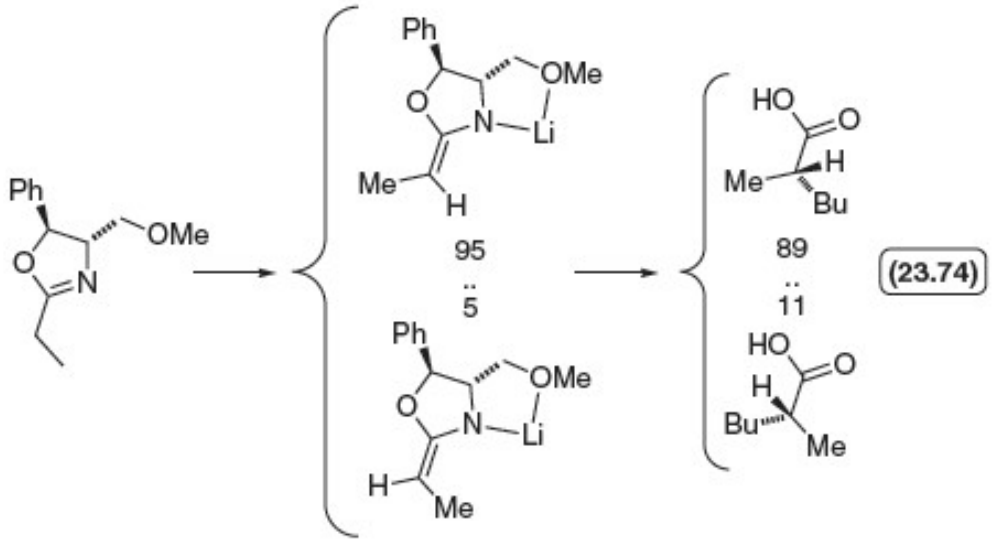

(23.74)

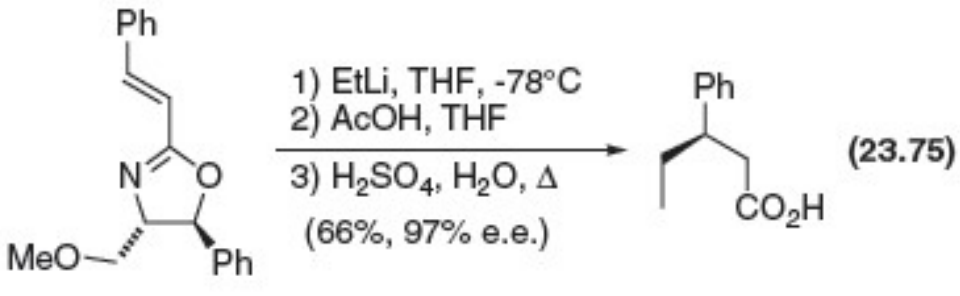

(23.75)

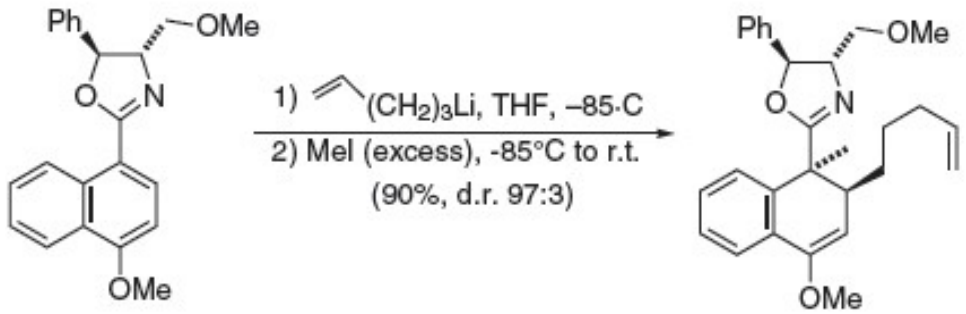

(23.76)

Asymmetric catalysts

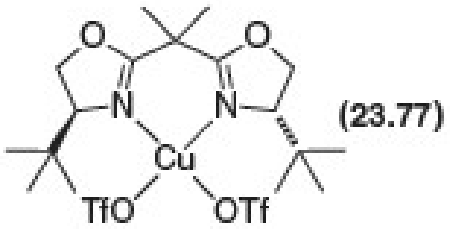

(23.77)

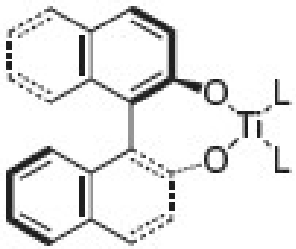

(23.78)

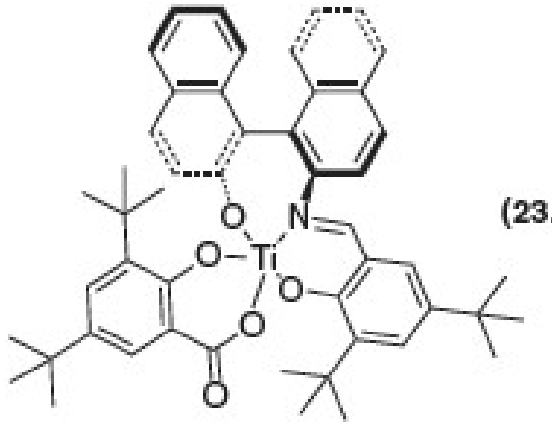

(23.79)

- chiral catalysts are almost always formed from an achiral precursor and a chiral ligand.
- chiral catalysts **23.77** and **23.78** are formed from the reaction between the chiral ligand and copper (II) triflate (**23.77**) or a titanium halide or alkoxide (**23.78**).
- common structural feature of many successful transition metal catalysts for asymmetric synthesis
  - presence of C_2-symmetric (or quasi-symmetric) ligands on the metal
  - entire catalyst has actual or approximate C_2 symmetry

Figure 23.19

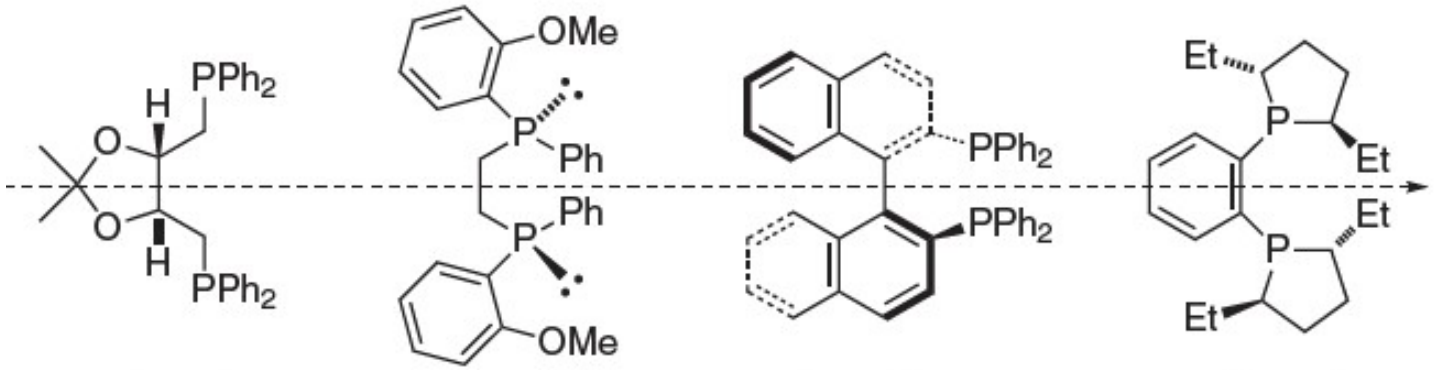

(23.80)
(*S*,*S*)-DIOP

(23.81)
(*R*,*R*)-DIPAMP

(23.82)
(*S*)-BINAP

(23.83)
(*R*,*R*)-Et-DuPHOS

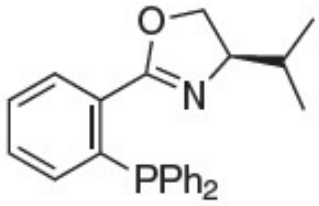

(23.84)
(*R*)-PHOX

- C_2-symmetric diphosphine ligands used in making asymmetric hydrogenation catalysts (top row). The C_2 axis common to these ligands is indicated by the dashed arrow.

Catalyzed dialkylzinc additions to aldehydes

- this catalyzed reaction gives product with very high e.e from a catalyst with low e.e.
- actual catalyst is dimeric
- the *meso* dimer is inactive as a catalyst
- the homochiral dimer is an active catalyst
- known as ***asymmetric amplification***

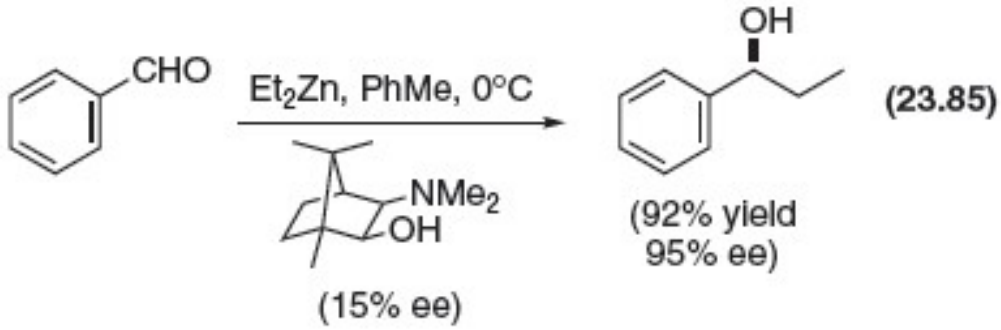

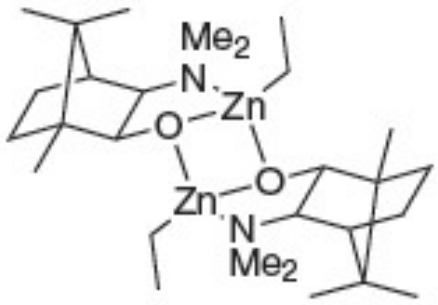

(23.86)
meso—inactive

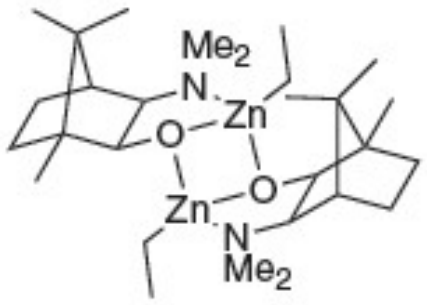

(23.87)
homochiral—active

Figure 23.20

- Non-linear effects in asymmetric reactions catalyzed by chiral adjuvants that are not enantiomerically pure

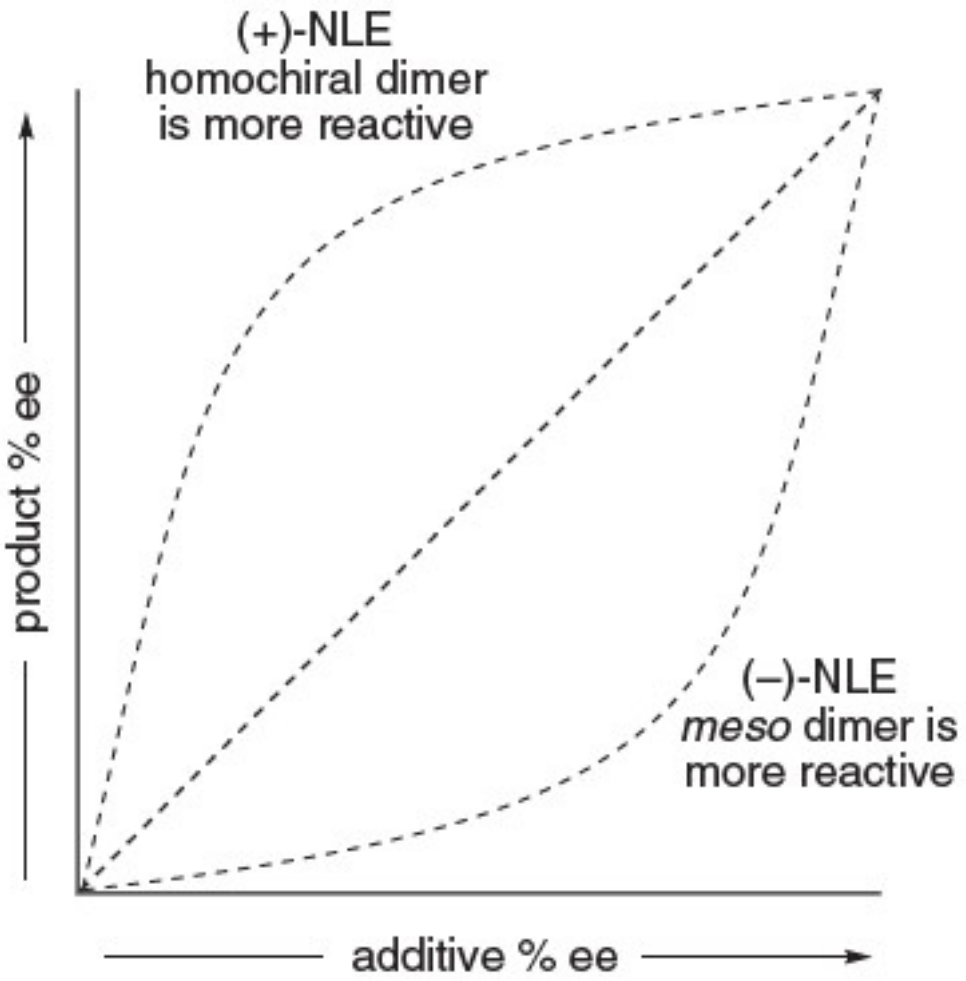

Chiral amplification with a chiral ytterbium catalyst

- when formed from the metal and ligand of relatively low e.e., the complex **23.88** appears to generate the homochiral form selectively.
- only the homochiral forms appears to be an active catalyst for the hetero-Diels-Alder reaction between Danishefsky's diene and benzaldehyde to give the chiral dihydropyran **23.89**.
- ligand with just 20% e.e. gave a product with the limiting value of 90% e.e.—the same level attained with optically pure catalyst in this system

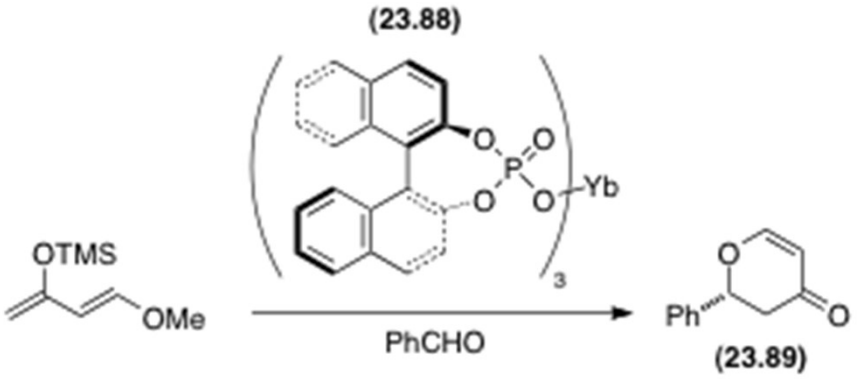

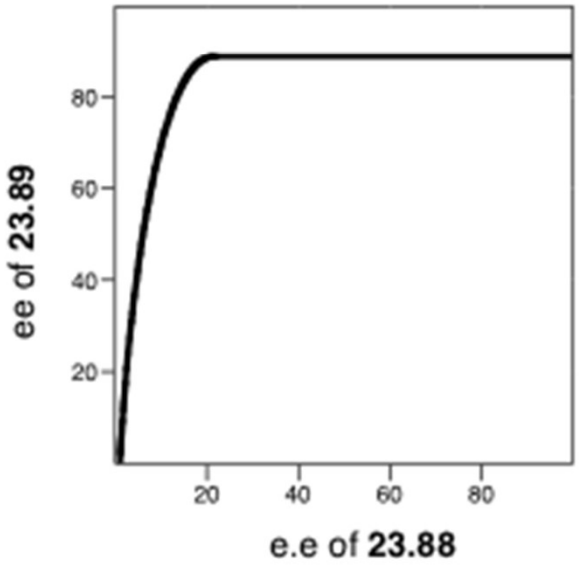

Asymmetric catalysis of the Diels-Alder reaction

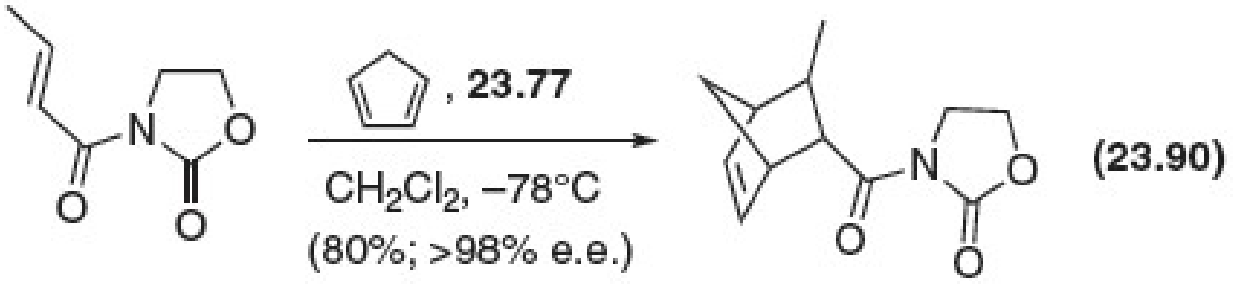

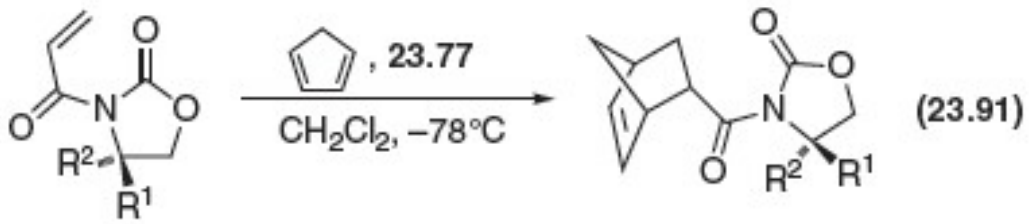

R^1= H, R^2 = CH_2Ph: 20% conversion, 36% e.e.
R^1= CH_2Ph, R^2 = H: 100% conversion, >99% e.e.

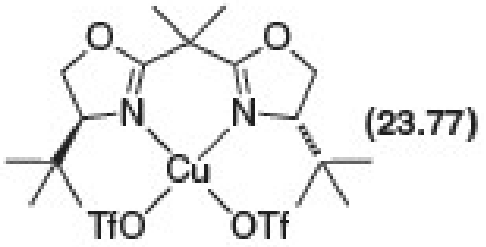

- Cu-BOX complex **23.77** catalyzes the Diels-Alder reaction of *N*-crotonyloxazolidinone
- replacing the achiral oxazolidinone with the chiral Evans oxazolidinone does not change the overall e.e. of the product or its absolute configuration
- the absolute configuration of the product is determined mainly by the chirality of the catalyst

Representative asymmetric catalytic aldol additions

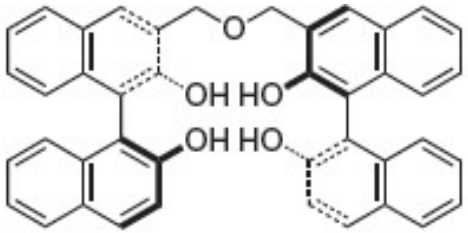

(23.92)

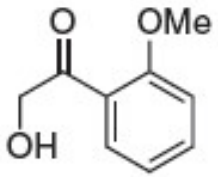

(23.94)

i-BuCHO, **23.92** (0.01 eq)

Et_2Zn (0.02 eq), THF, –30°C

(84%)

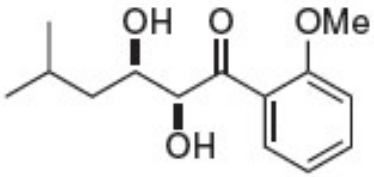

(23.95)

+

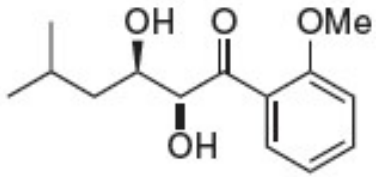

(23.96

dr:	84	:	16
ee:	93%		87%

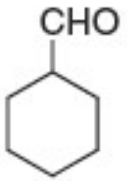

Et_2Zn (0.1 eq)
22.97 (0.05 eq)

PhCOMe (10 eq)
4Å MS, THF

(60%; 98% ee)

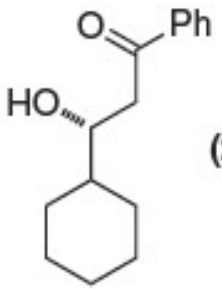

(22.98)

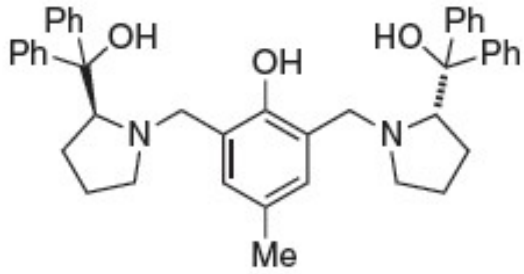

(23.97)

Figure 23.21

- Basic activation of a carbonyl group by chiral catalysis

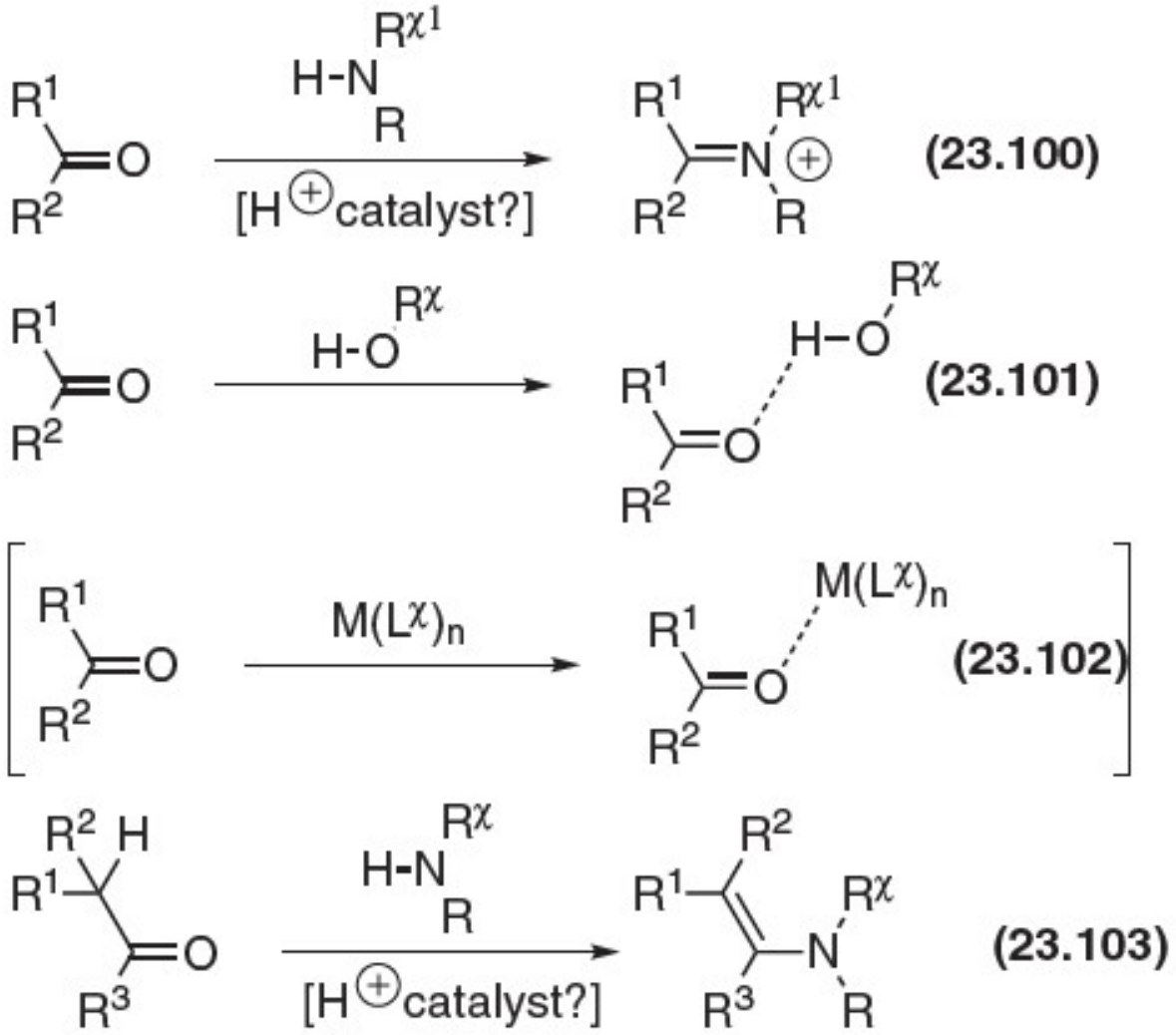

Organocatalysis of the aldol addition by proline

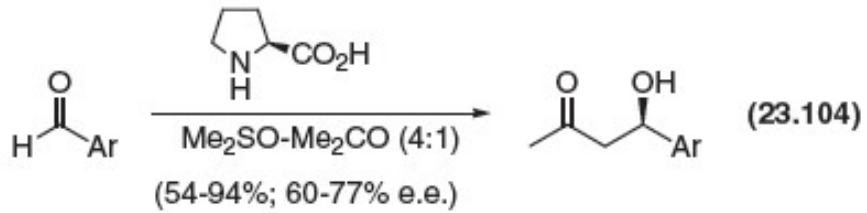

(23.104)

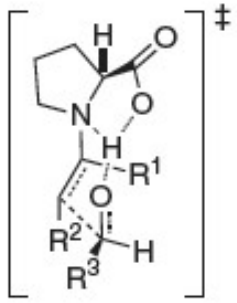

(23.105)

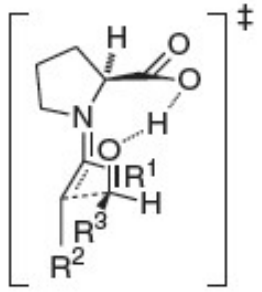

(23.106)

both nucleophilic (the secondary amine) and electrophilic (the carboxylic acid) groups are essential for good organocatalyst reactivity

Proline-based organocatalysts

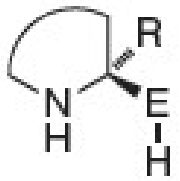

(23.107)

ring size: usually 5
E = O, ArO, CO_2, CONR, $(RO)_2PO_2$, $RO(R)PO_2$, R_2PO_2, CR_2NCOR, CR_2NSO_2R

- structural features of successful organocatalysts for the aldol addition

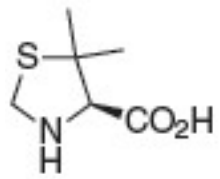

(23.108)

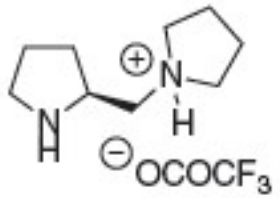

(23.109)

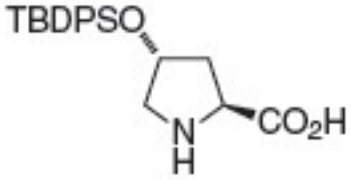

(23.110)

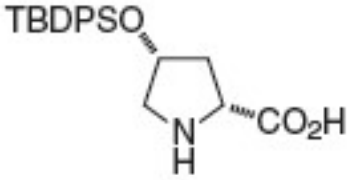

(23.111)

- proline analogs useful as organocatalysts for the aldol addition

Figure 23.22

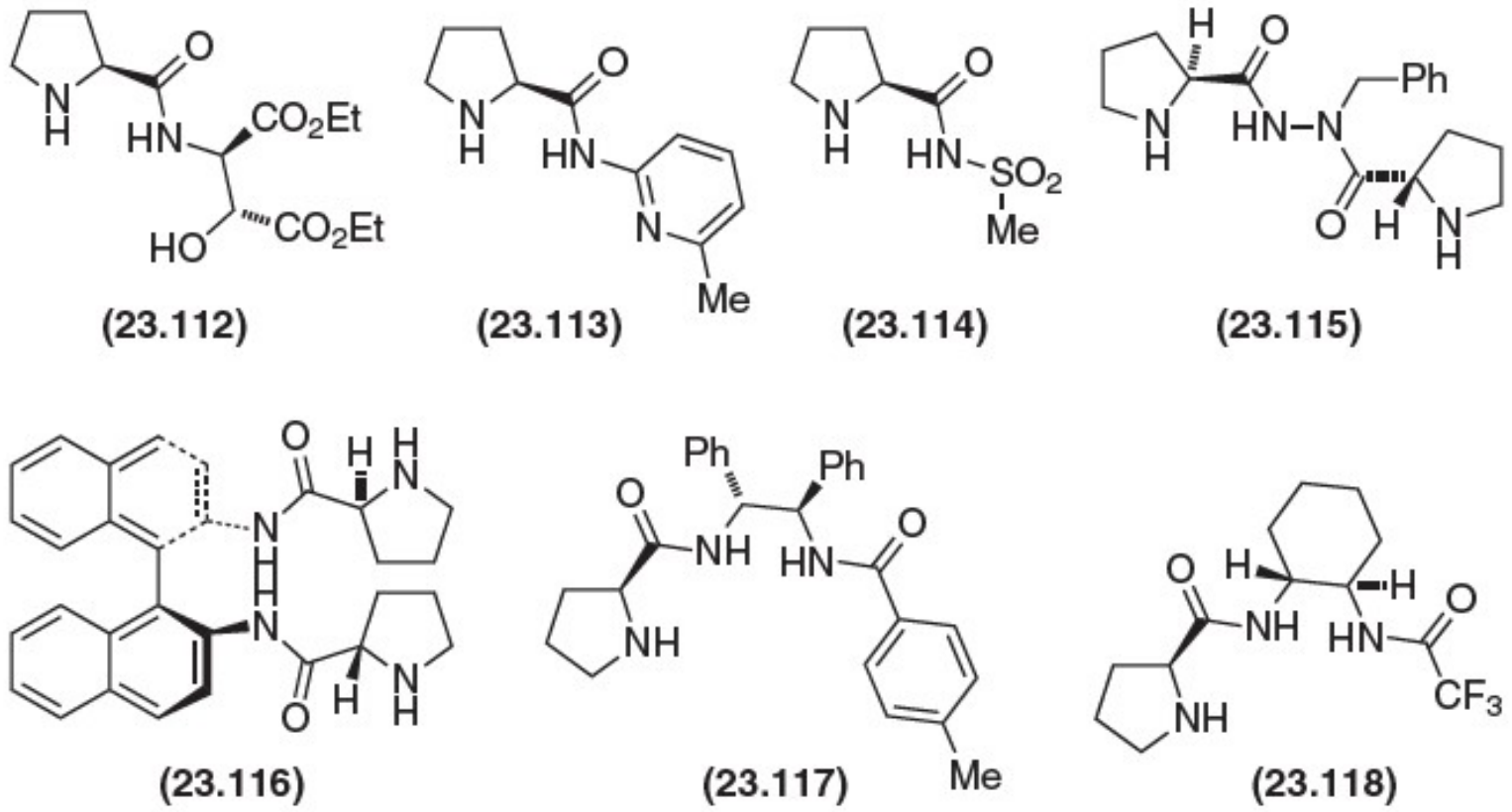

- Proline amide organocatalysts for aldol additions in aqueous solution

MacMillan imidazolidinones as organocatalysts

- the function of the amide groups in aligning the pyruvic acid in the aldol addition reaction with a methyl ketone (**23.119**)
- the prototypical MacMillan chiral imidazolidinone (**23.120**)
- use of **23.120** as an organocatalyst for the Mukaiyama-type addition to a silyloxyfuran
- a model for the reactive conformation of an iminium ion based on the MacMillan imidazolidinone

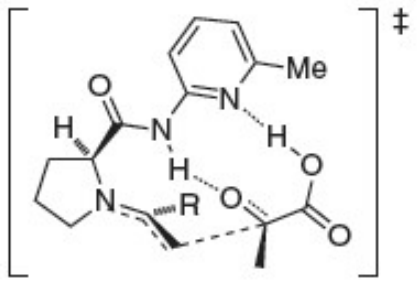

(23.119)

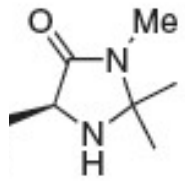

(23.120)

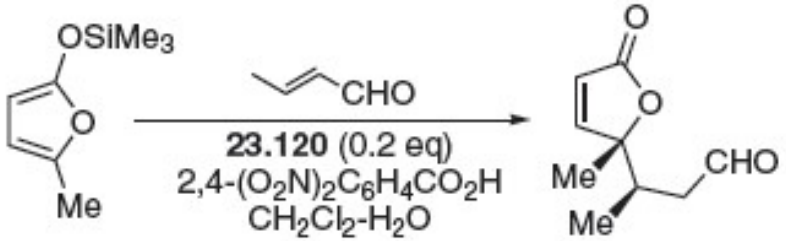

(23.121)

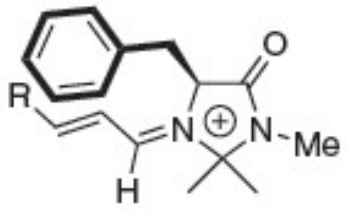

(23.122)

The enantioselective total synthesis of salicylihalamides A and B

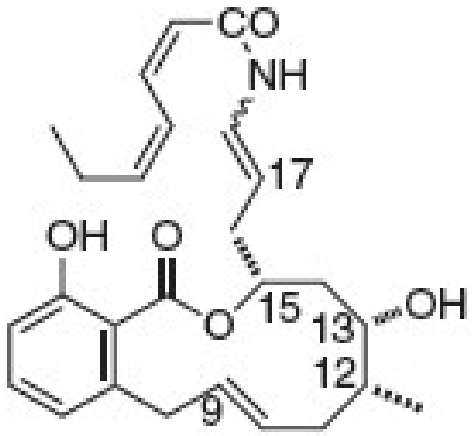

(23.123)

Figure 23.23

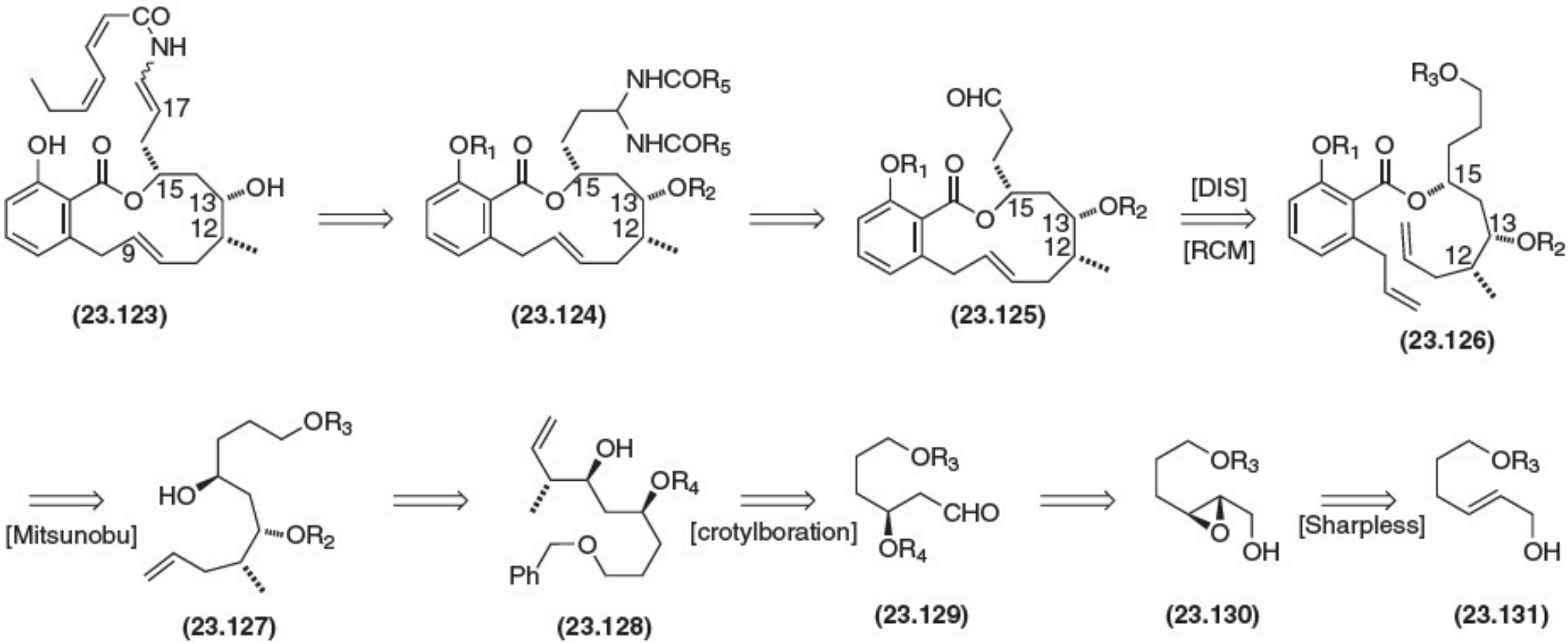

The retrosynthetic analysis of the salicylihalamides

Figure 23.24 (a)

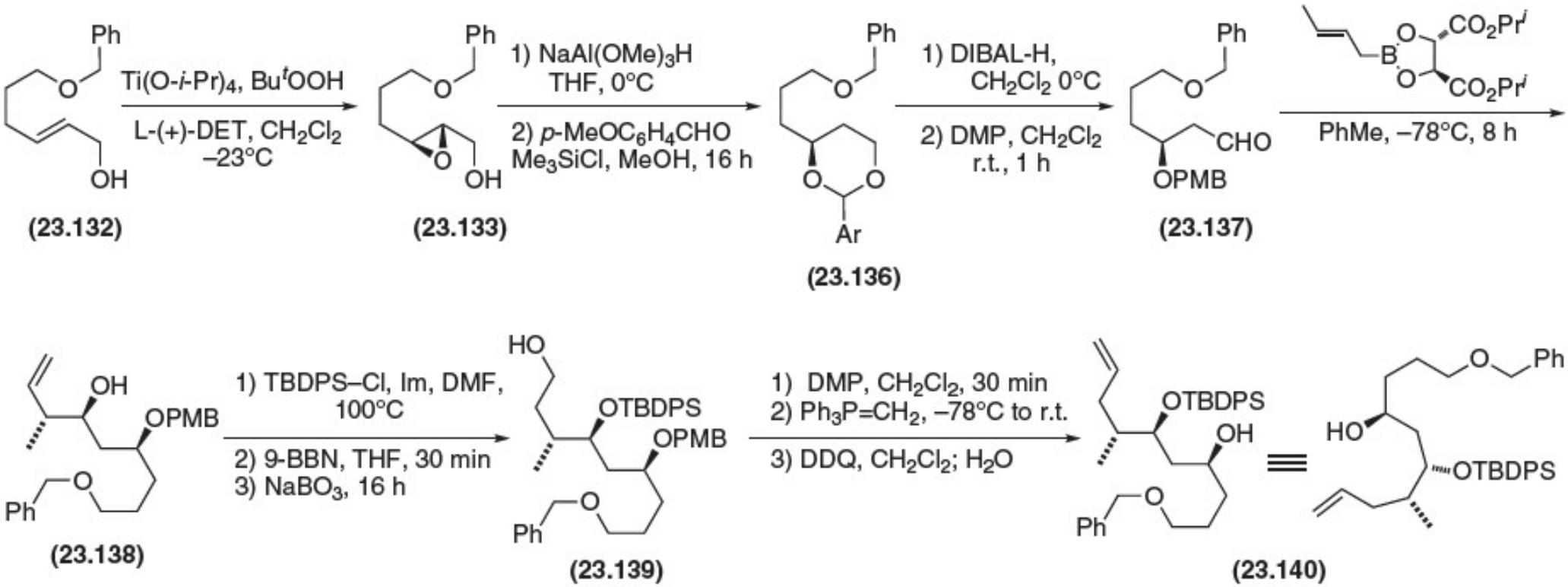

- The synthesis of salicylihalamides A and B (part 1)

Figure 23.24 (b)

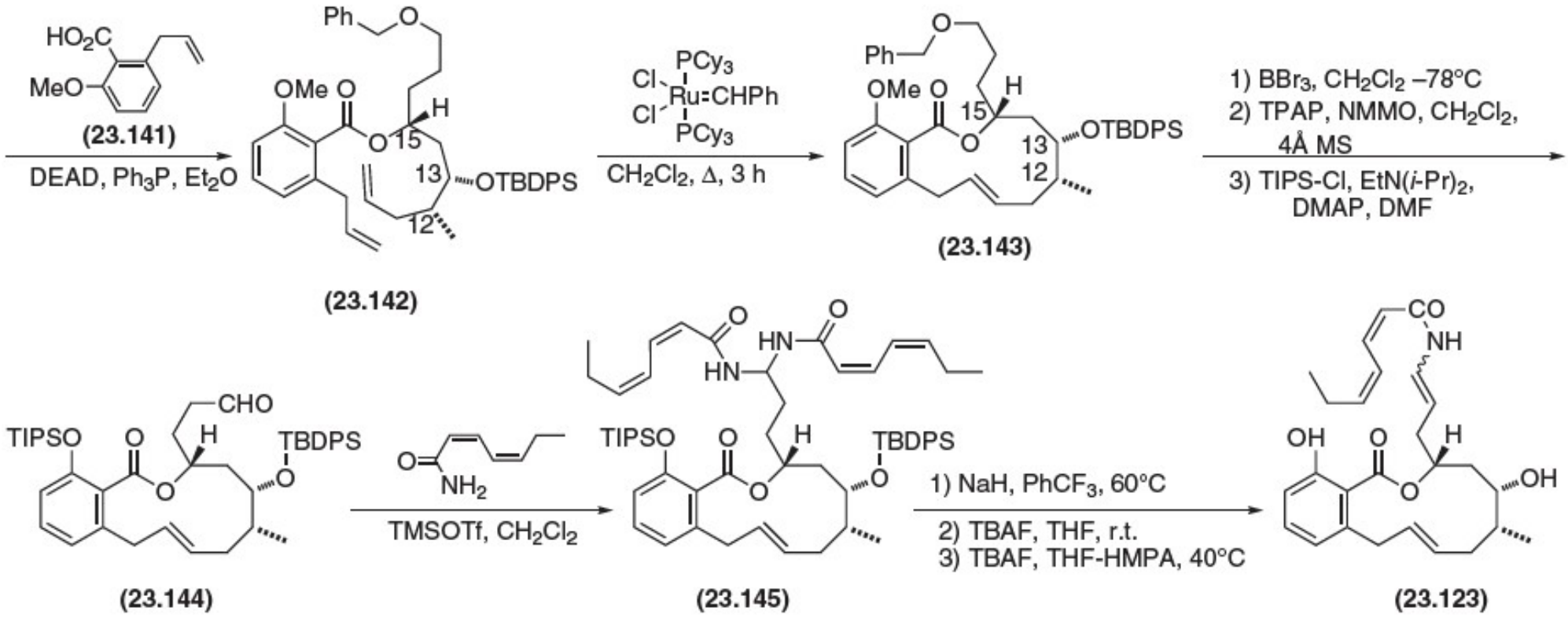

- The synthesis of salicylihalamides A and B (part 2)

Figure 23.25

- regiospecific epoxide ring opening

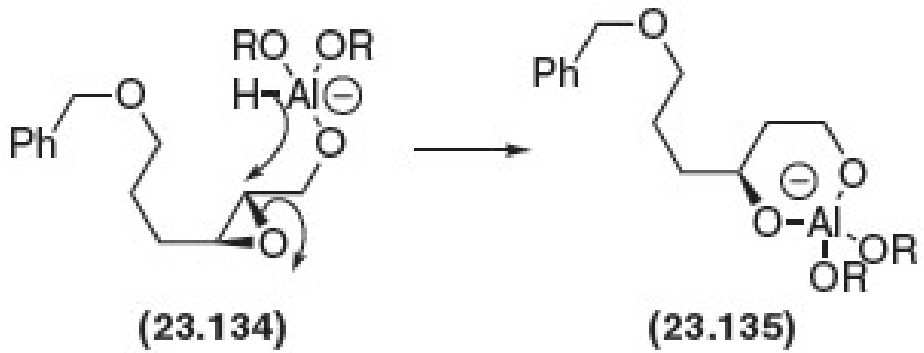

(23.134) (23.135)

DIBAL-H reduction of the acetal **23.136**

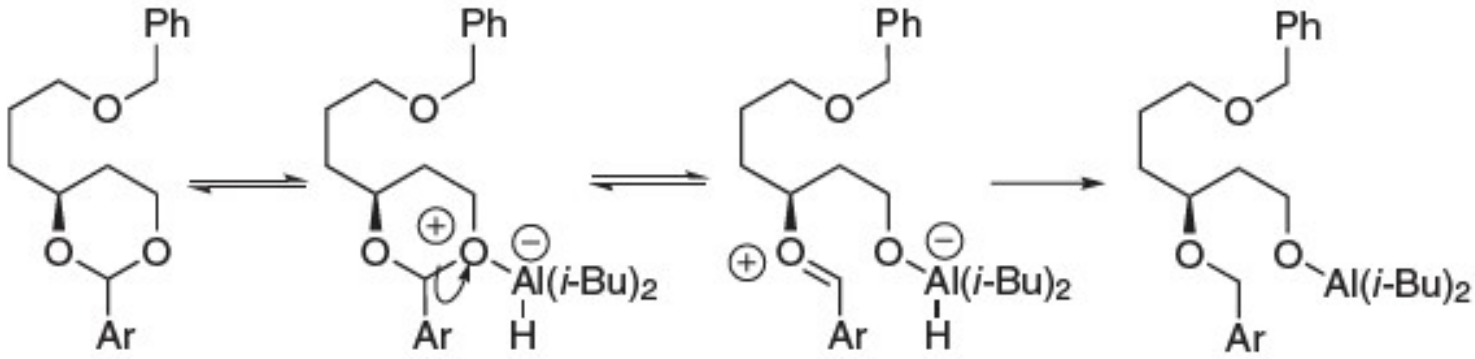

(23.136) (23.146) (23.147) (23.148)

The enantioslective synthesis of aigialomycin D

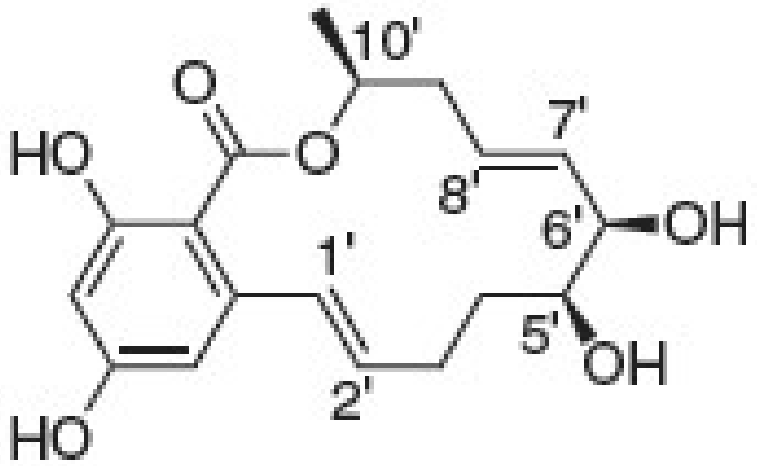

(23.149)

Figure 23.26

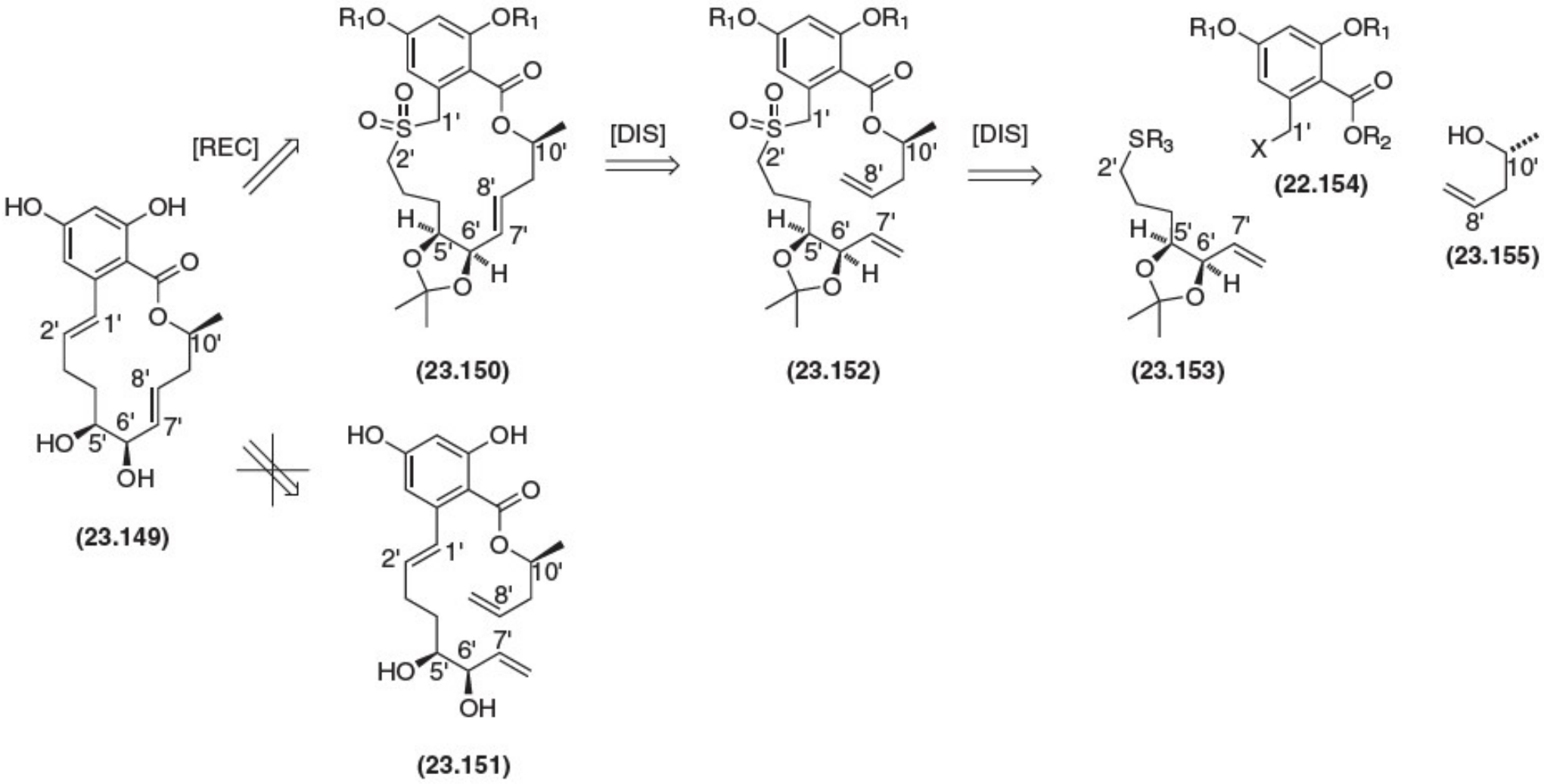

Retrosynthetic analysis of the Harvey synthesis of aigialomycin

Figure 23.27

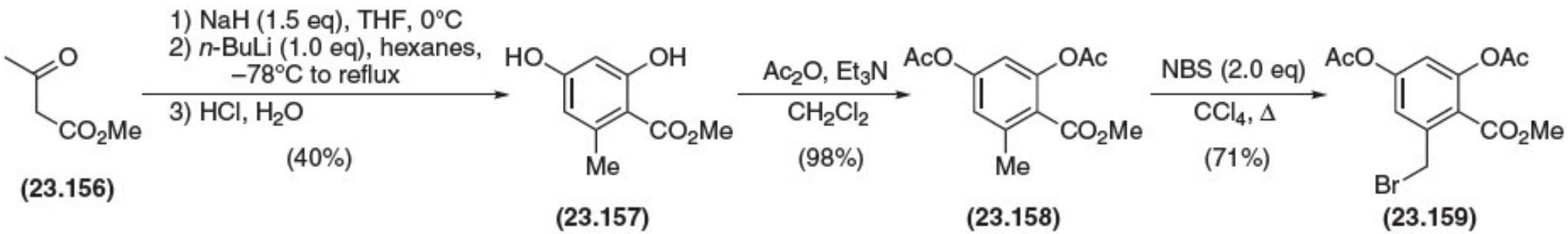

- Synthesis of the orsellinic acid synthon

Figure 23.28

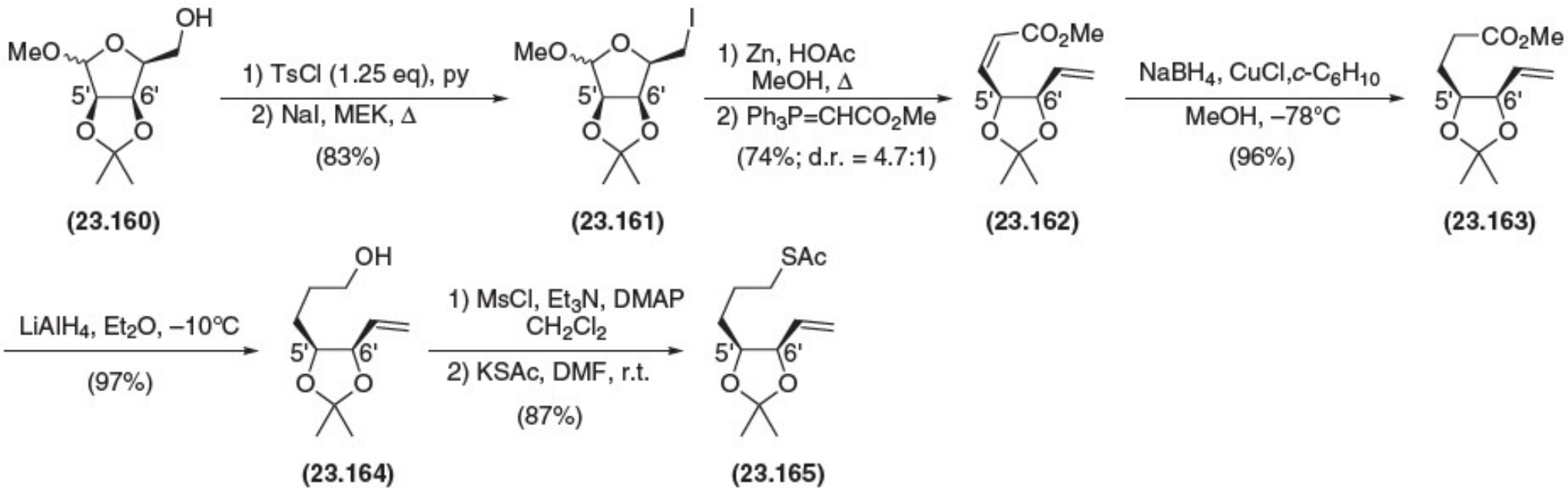

- Synthesis of the ribose-based thiol synthon

Figure 23.29

Completion of the synthesis of aigialomycin

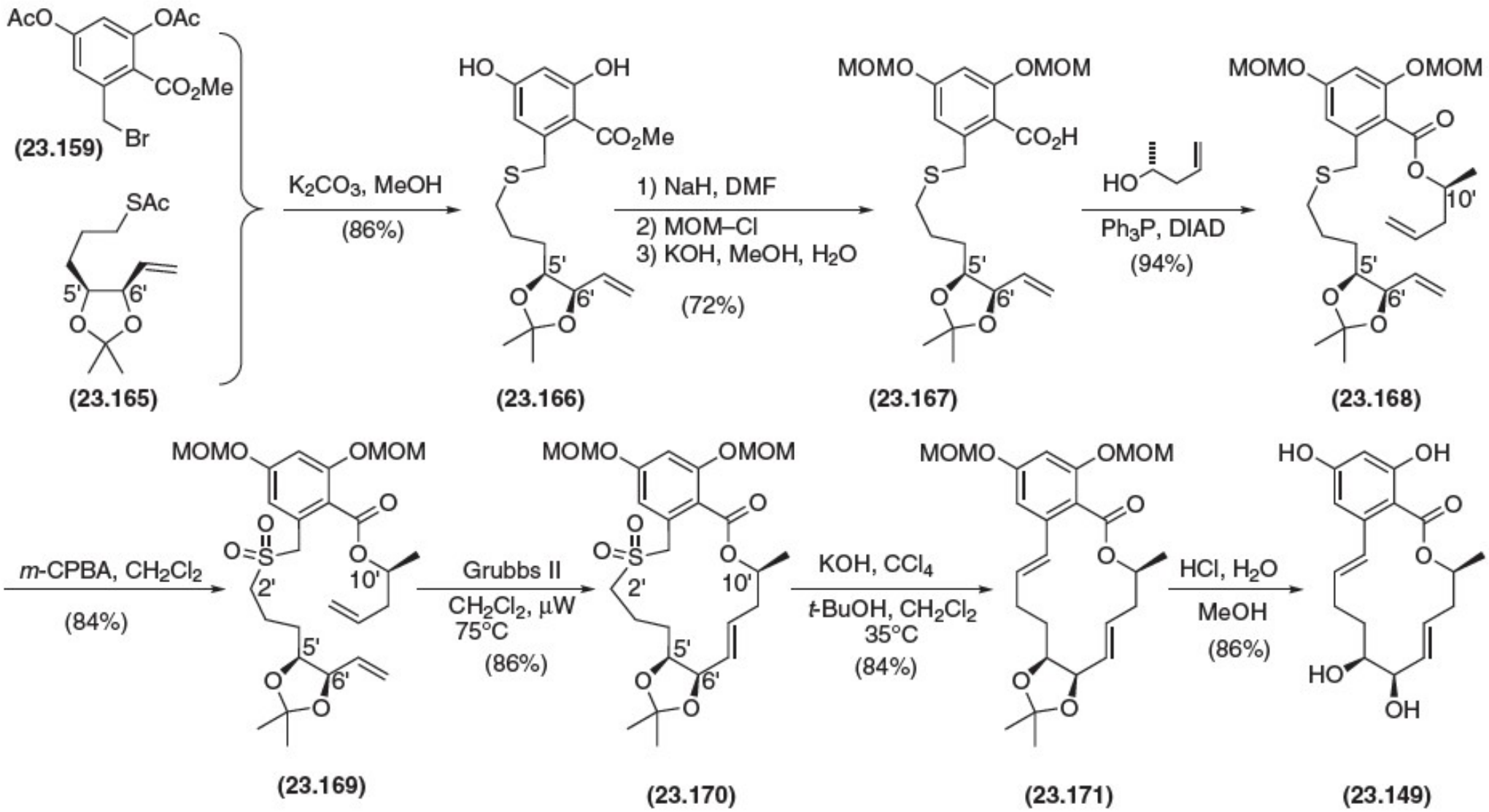

The enantioselective synthesis of chinesiolide B

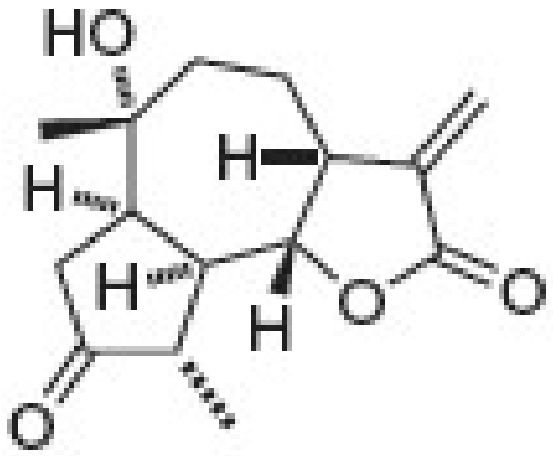

(23.172)

Figure 23.30

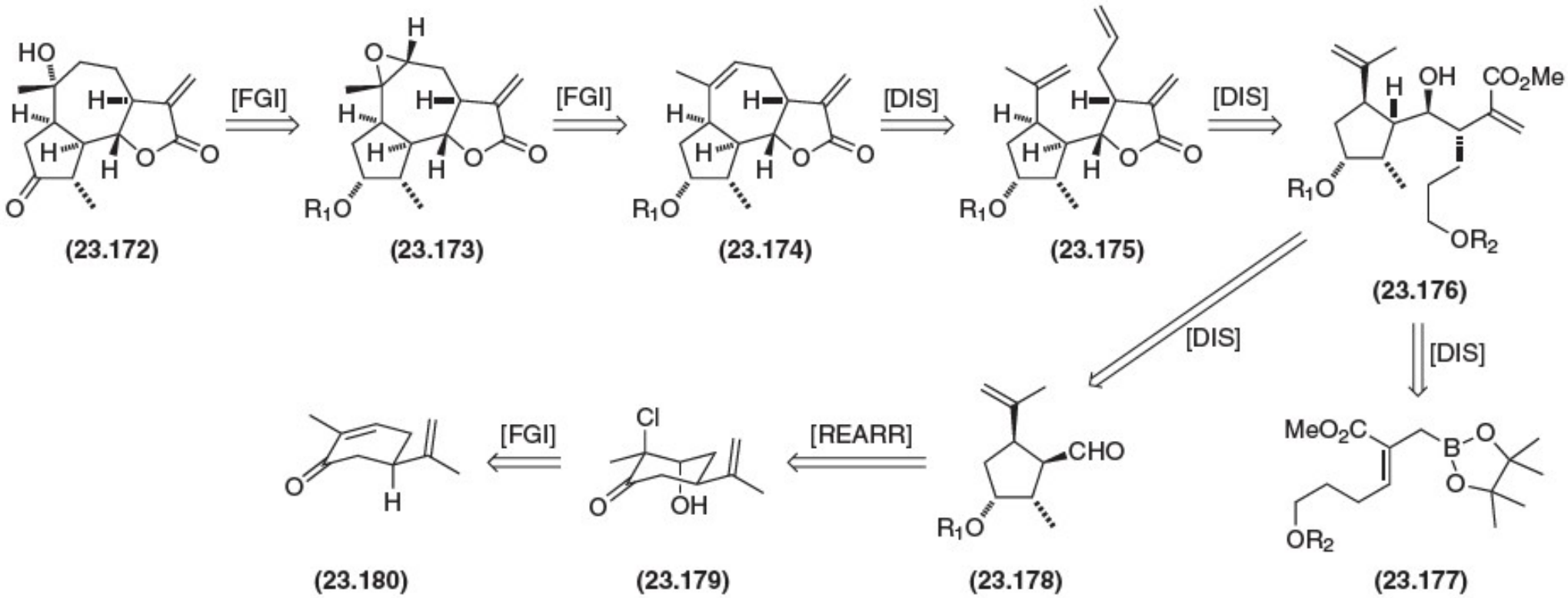

- Retrosynthetic analysis of chinensiolide B

Figure 23.31 (a)

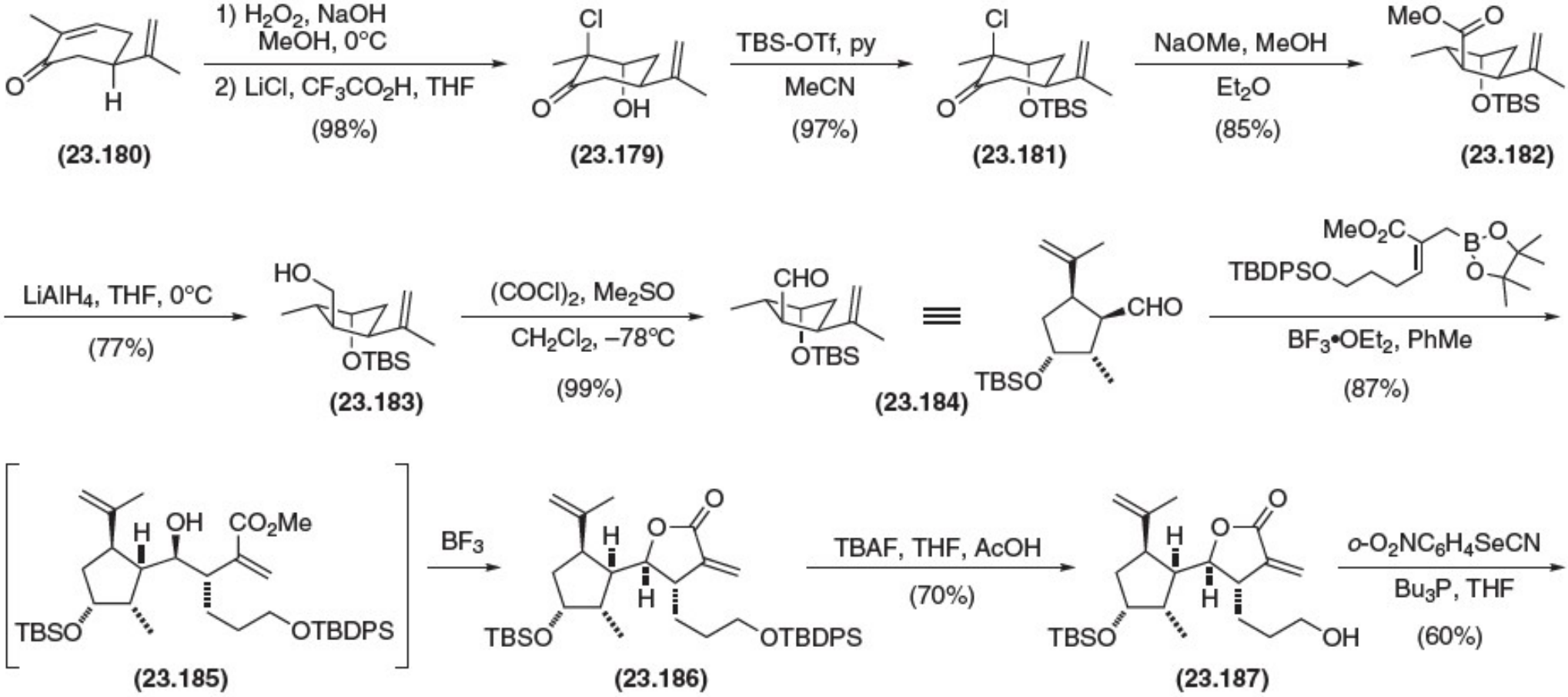

- The synthesis of chinensolide B (Part 1)

Figure 23.31 (b)

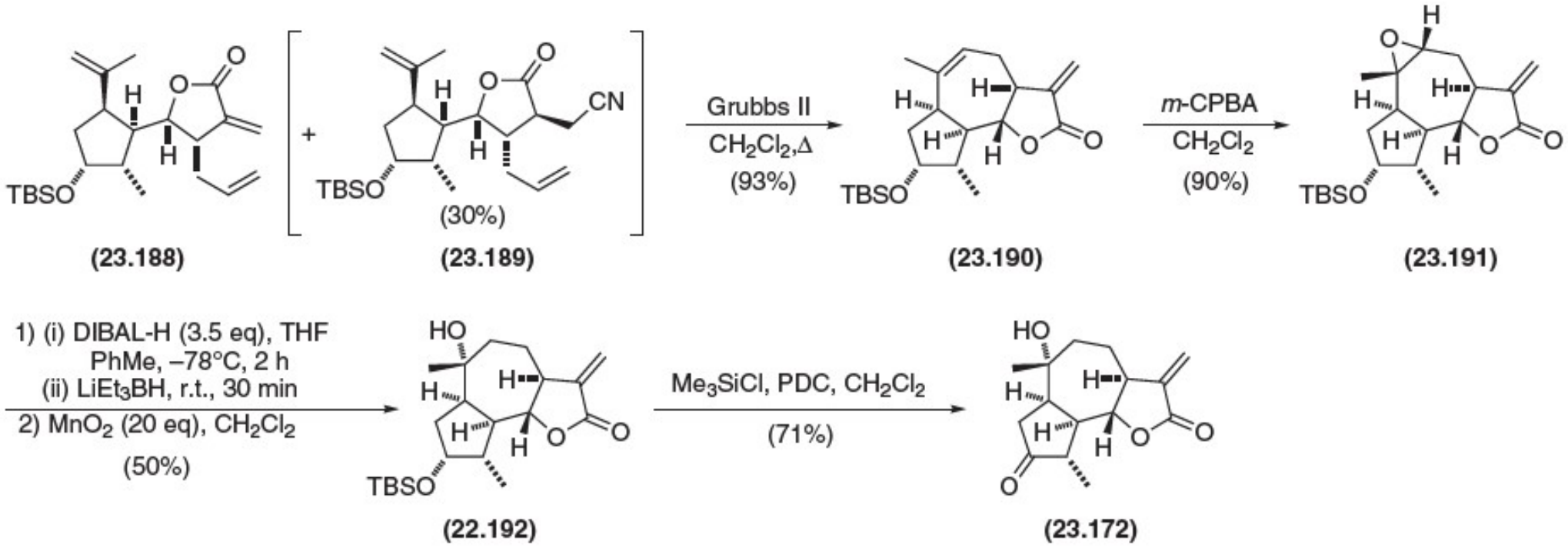

- The synthesis of chinensolide B (Part 2)

Key ring closing metathesis

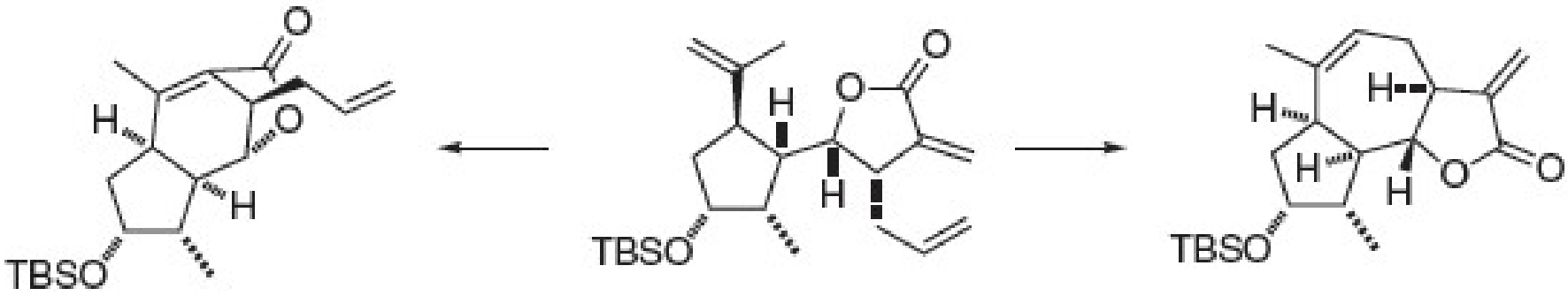

(23.193) (23.188) (23.190)

- there are at least two potential ways for the ring-closing metathesis reaction to occur.
- The more reactive alkene π bond, from the α-methylene lactone could react to form a six-membered ring (**23.193**), or
- the terminal π bond of the side chain may react to form the seven-membered ring (**23.190**). Only compound **23.190** is formed.

The enantioselective synthesis of plakortethers F and G

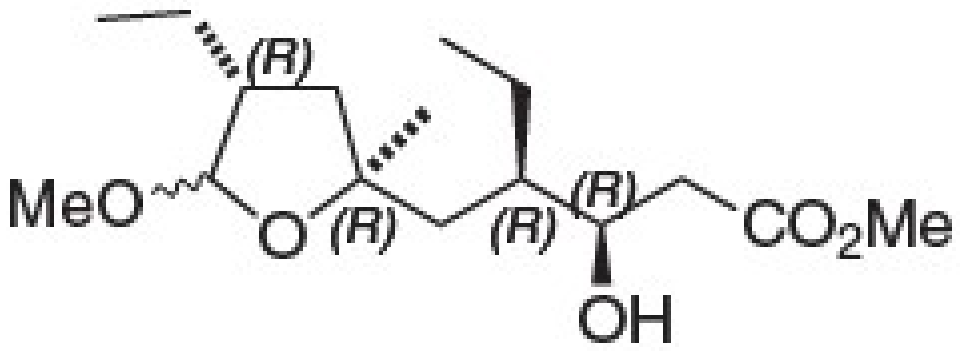

(23.194)

Figure 23.32

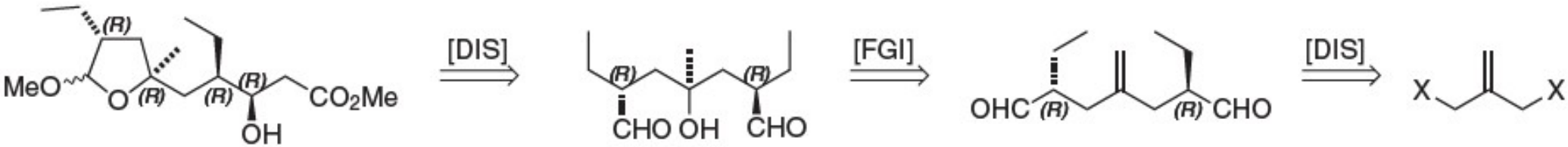

(23.194) (23.195) (23.196) (23.197)

Simplified retrosynthetic analysis of plakortethers F and G

Figure 23.33 (a)

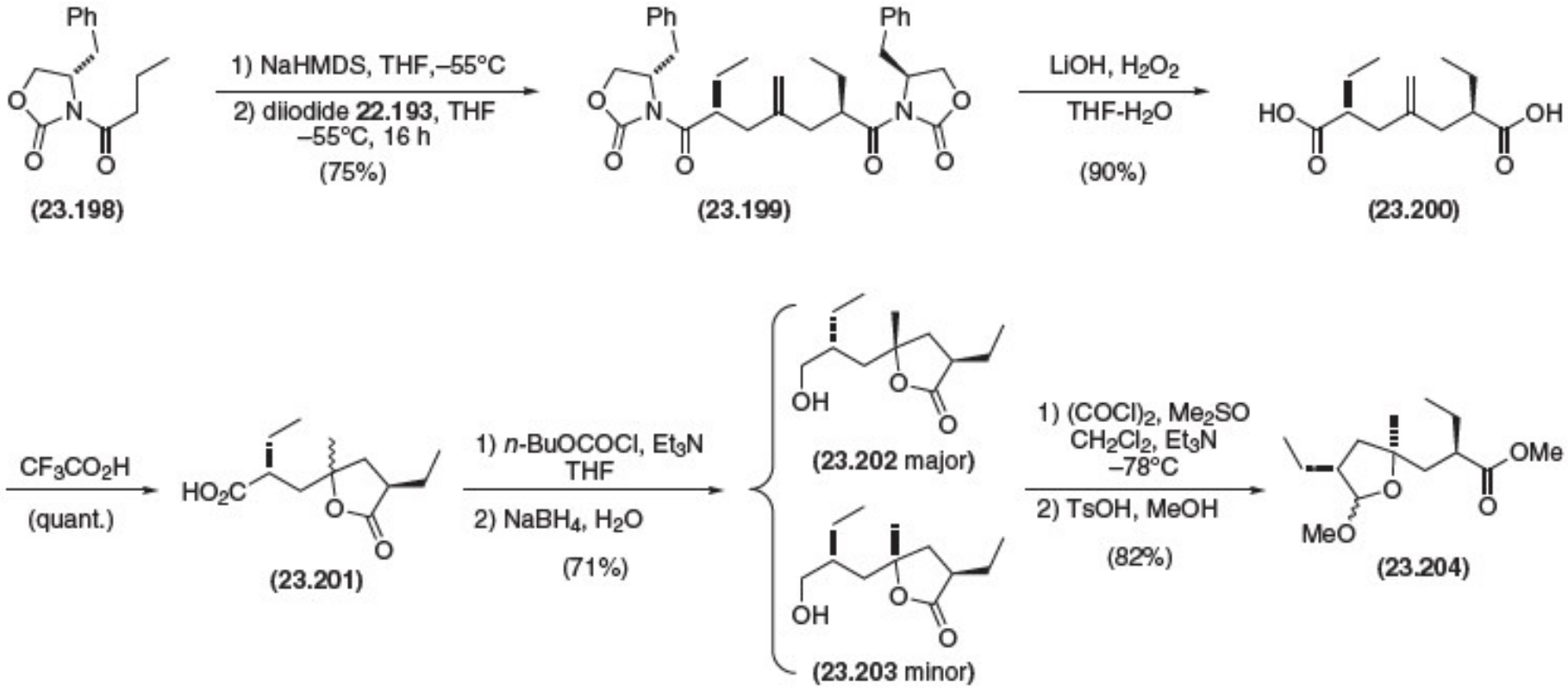

- The total synthesis of plakortethers F and G (Part 1)

Figure 23.33 (b)

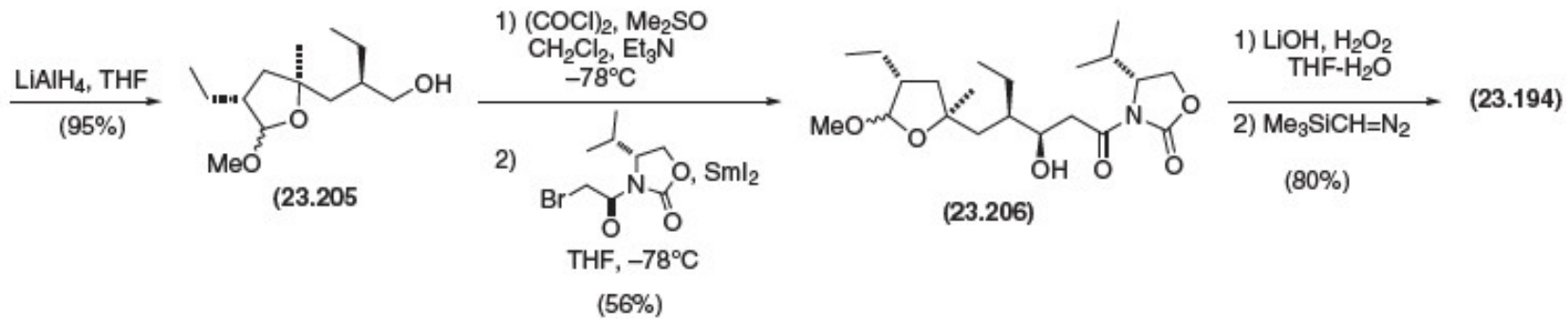

- The total synthesis of plakortethers F and G (Part 2)

The asymmetric synthesis of a proposed structure of iriomoteolide-1b

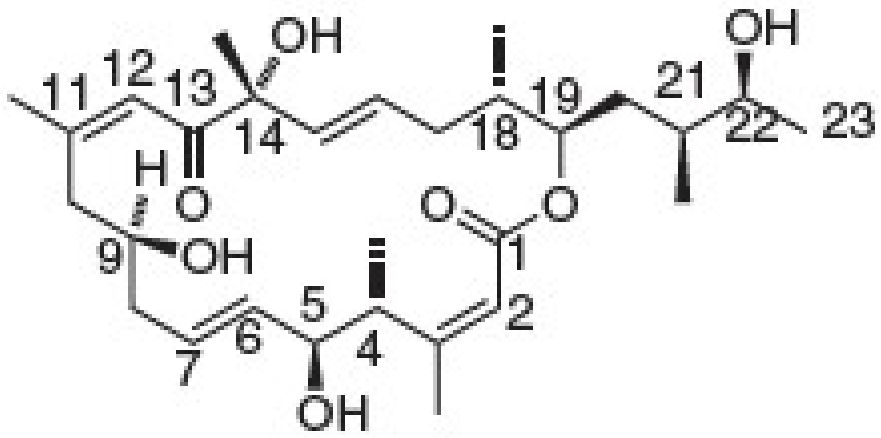

(23.207

Figure 23.34

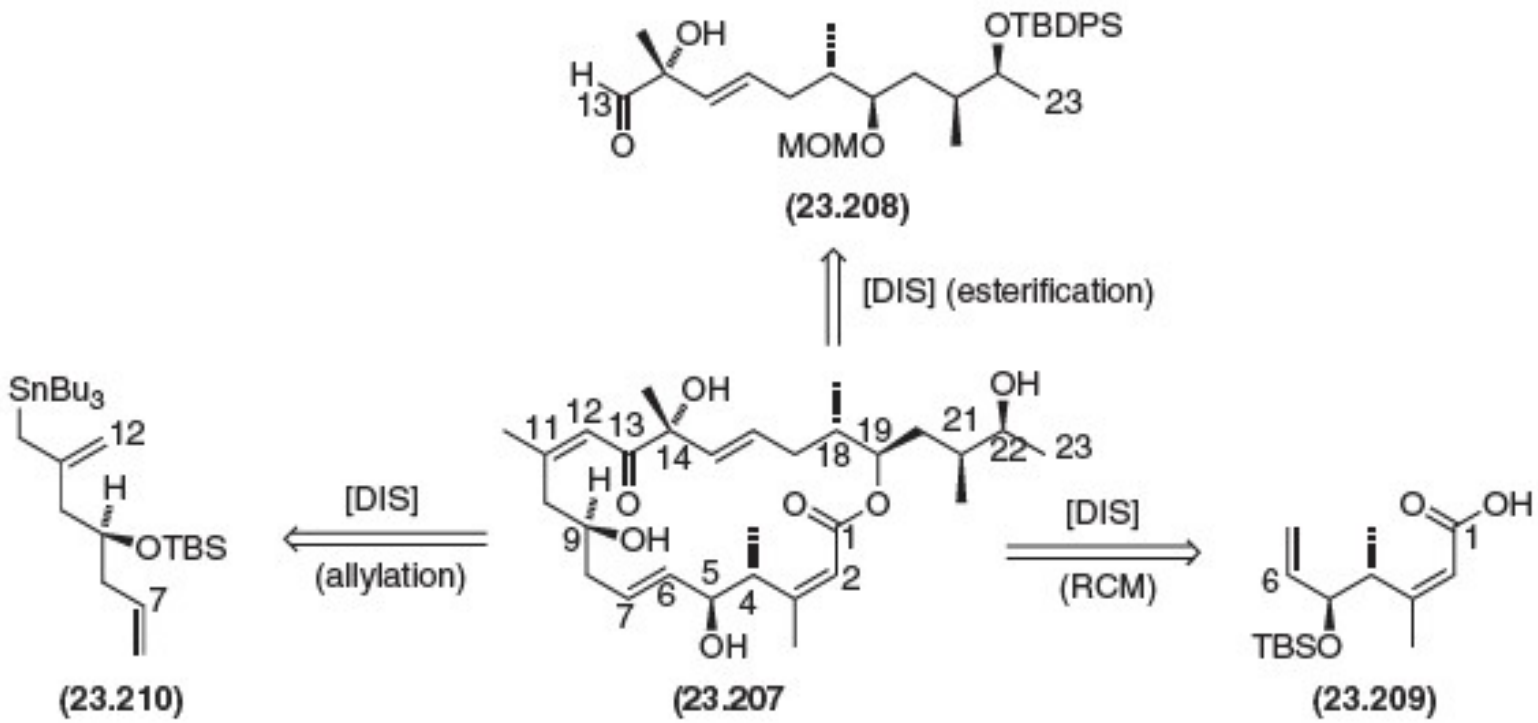

- Major disconnections of the iriomoteoilide-1b molecule

Figure 23.35

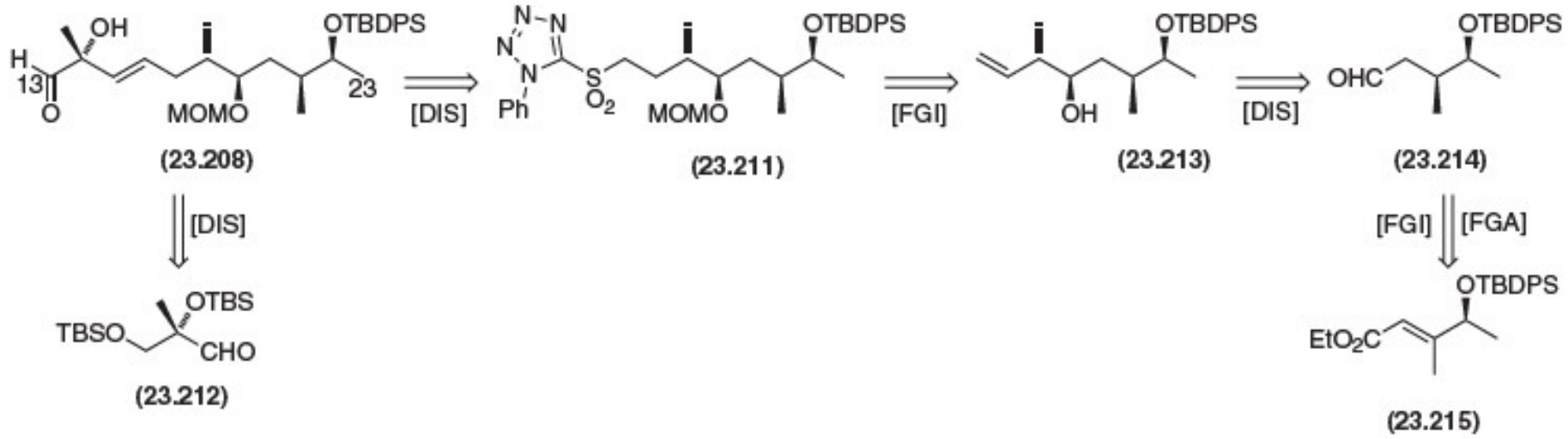

- The retrosynthetic analysis of synthon **23.208**

Figure 23.36 (a)

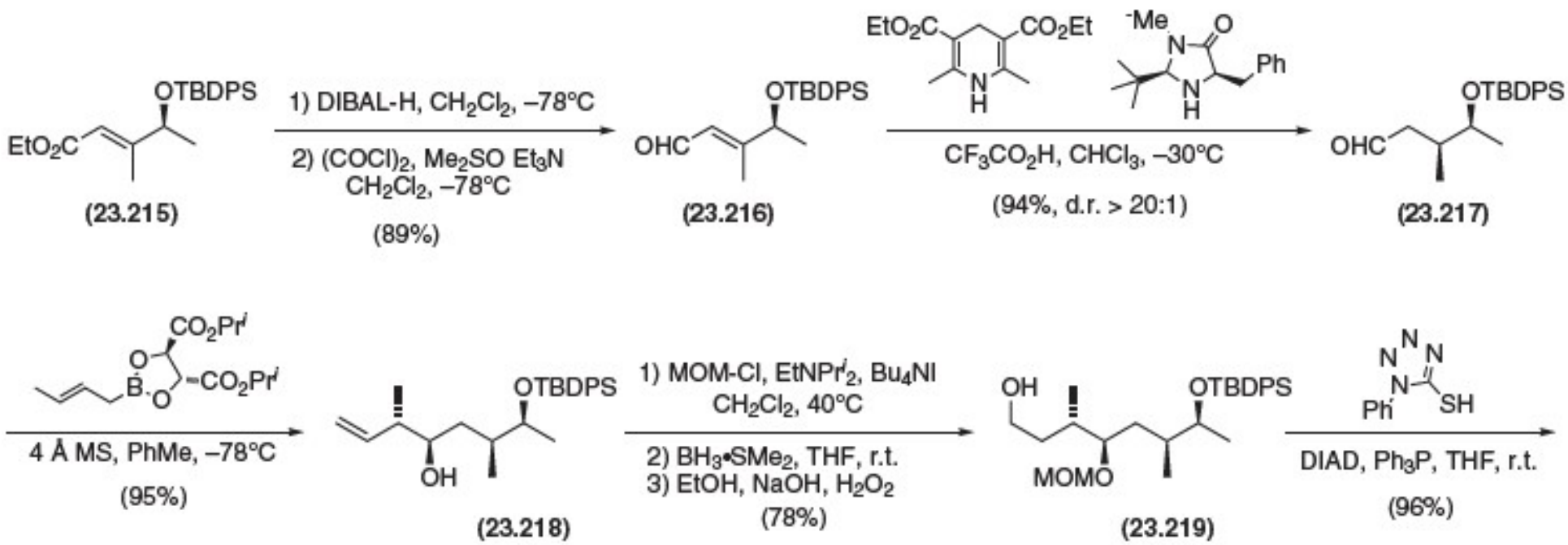

- The synthesis of synthon **23.208** (Part 1)

Figure 23.36 (b)

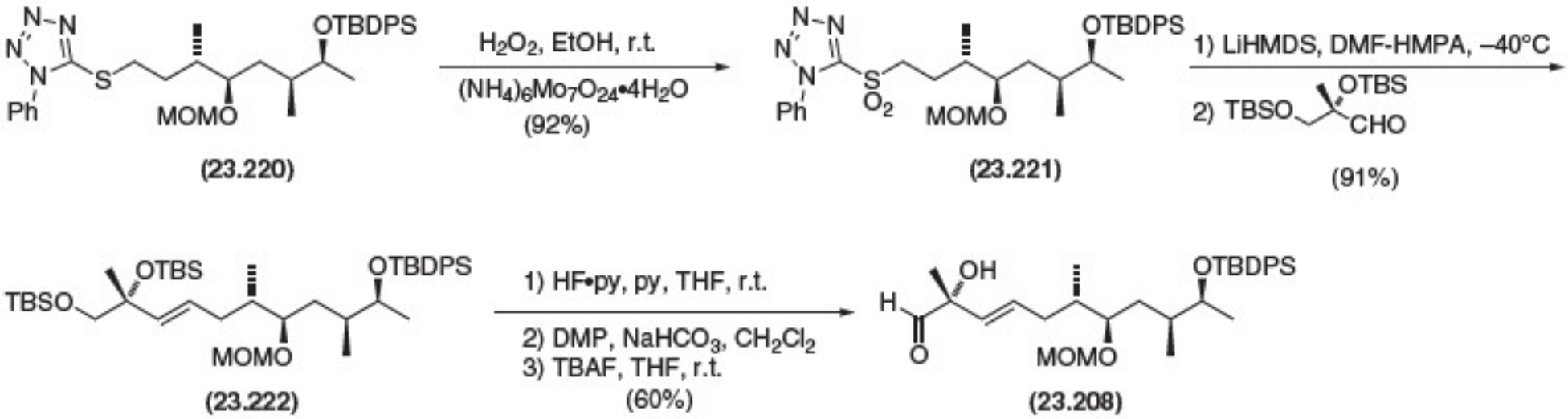

- The synthesis of synthon **23.208** (Part 2)

Figure 23.37

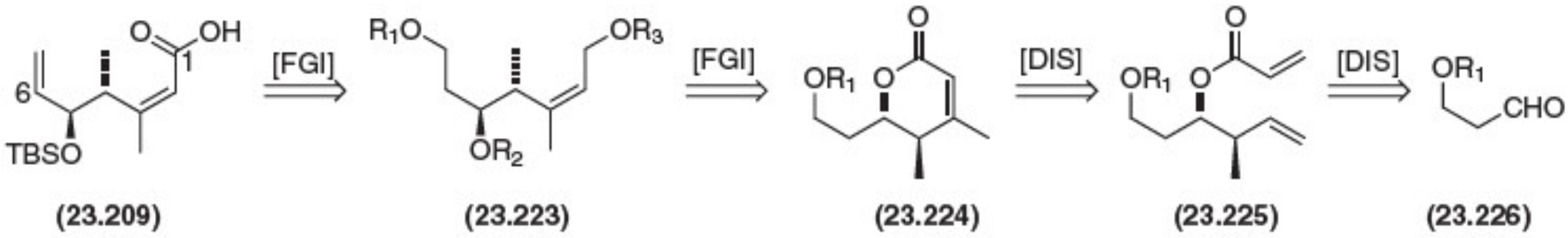

(23.209) (23.223) (23.224) (23.225) (23.226)

- Retrosynthetic analysis of synthon **23.209**

Figure 23.38

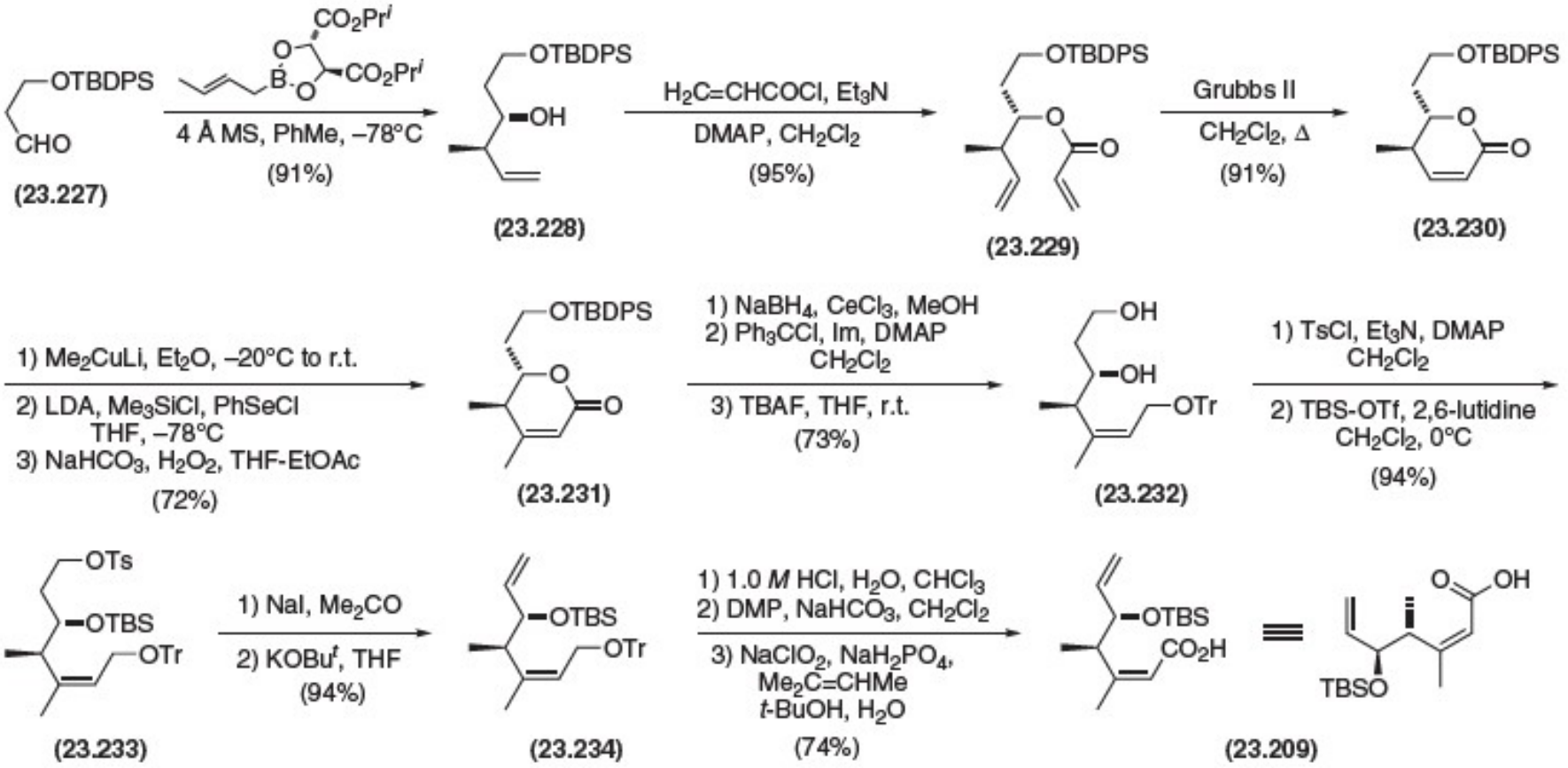

- The synthesis of the C1-C6 synthon **23.209**

Figure 23.39

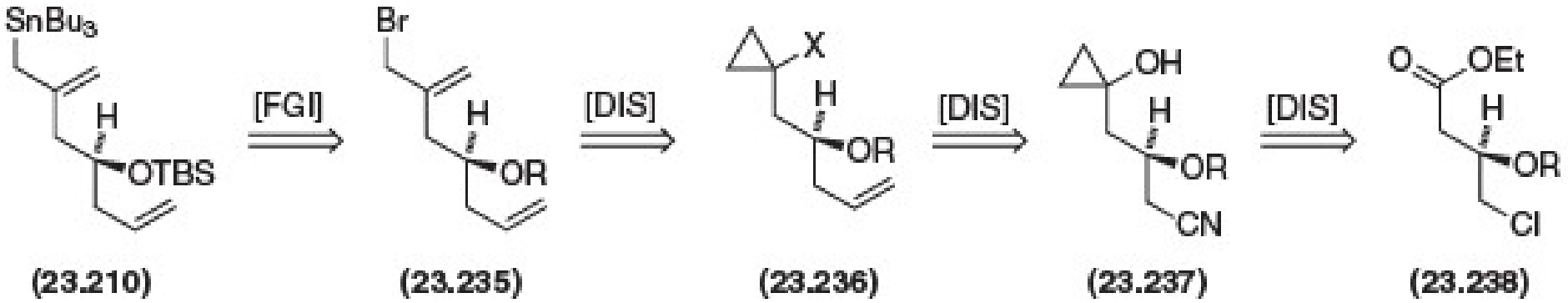

(23.210) (23.235) (23.236) (23.237) (23.238)

The retrosynthetic analysis of the C7-C12 allylstannane synthon **23.210**

Figure 23.40

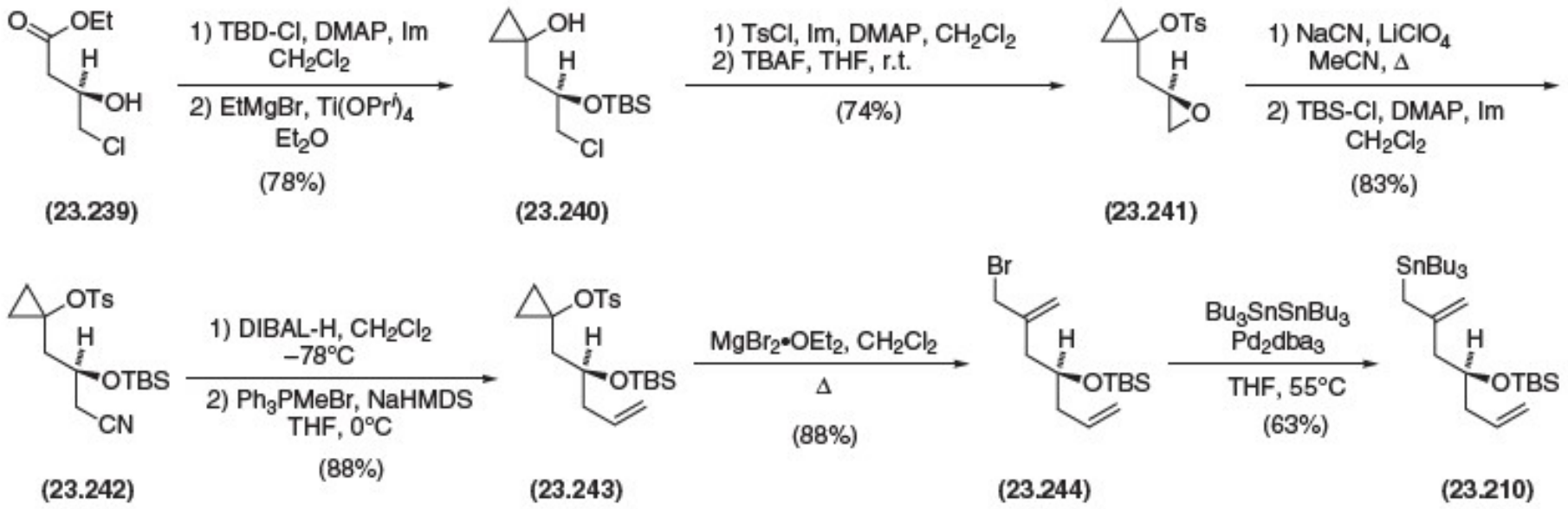

- Synthesis of the C7-C12 allylstannane synthon **23.206**

Figure 23.41

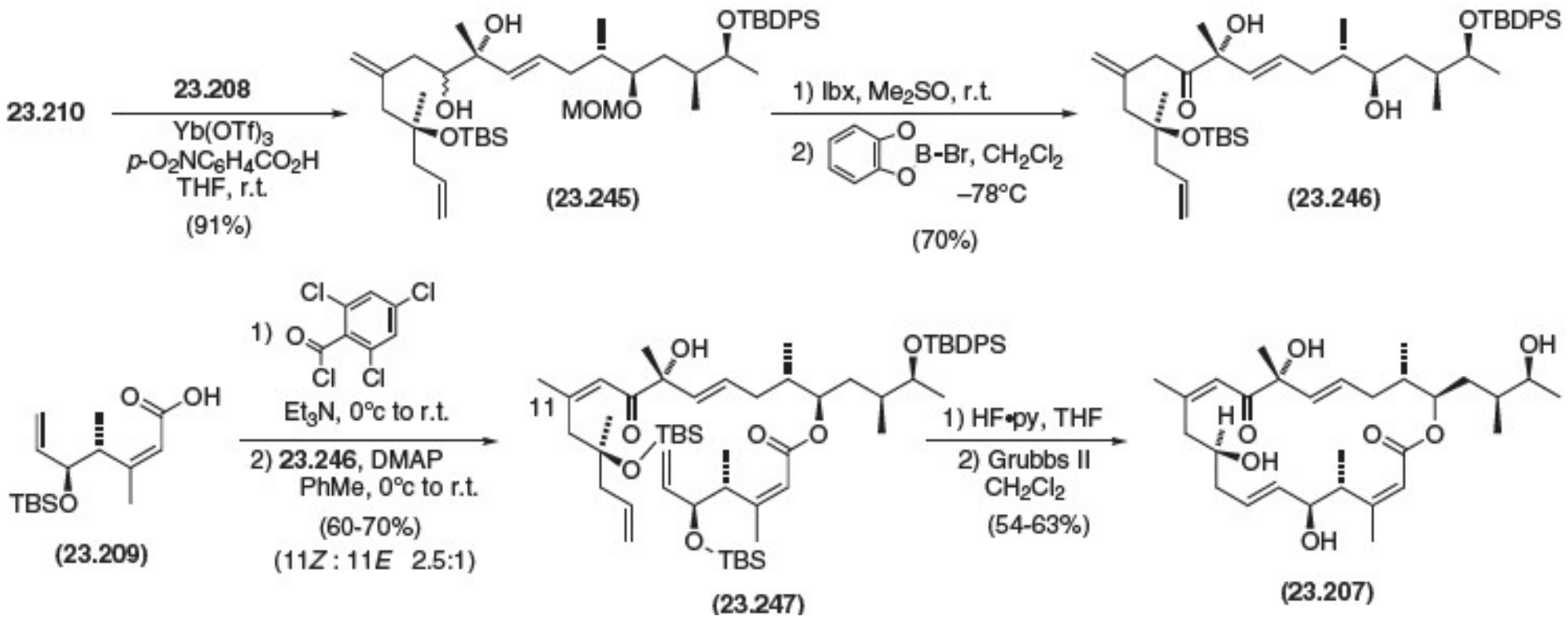

Completion of the synthesis of the structure proposed for iriomoteolide-1b

An enantioselective synthesis of manzacidin-C

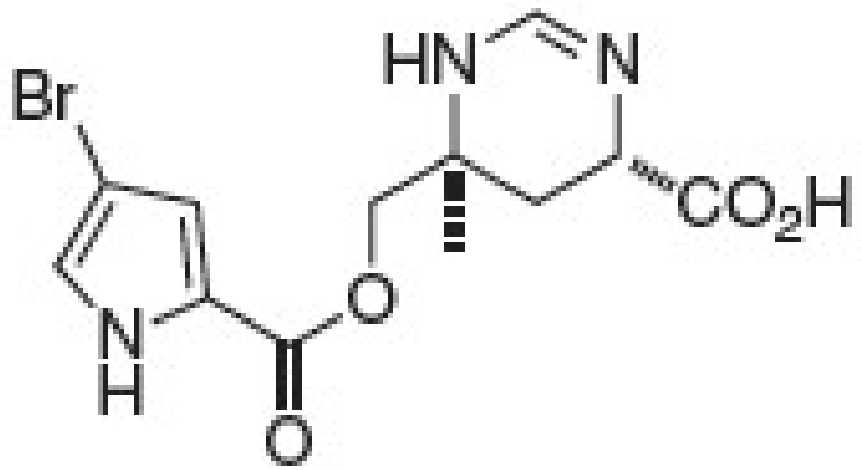

(23.248)

Figure 23.42

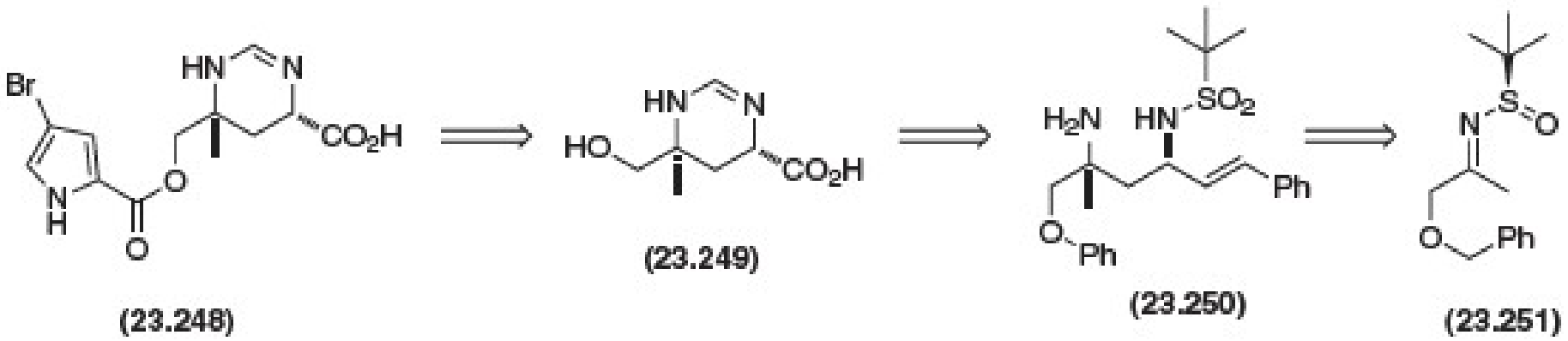

- Retrosynthetic analysis of manzacidin-C

Figure 23.43

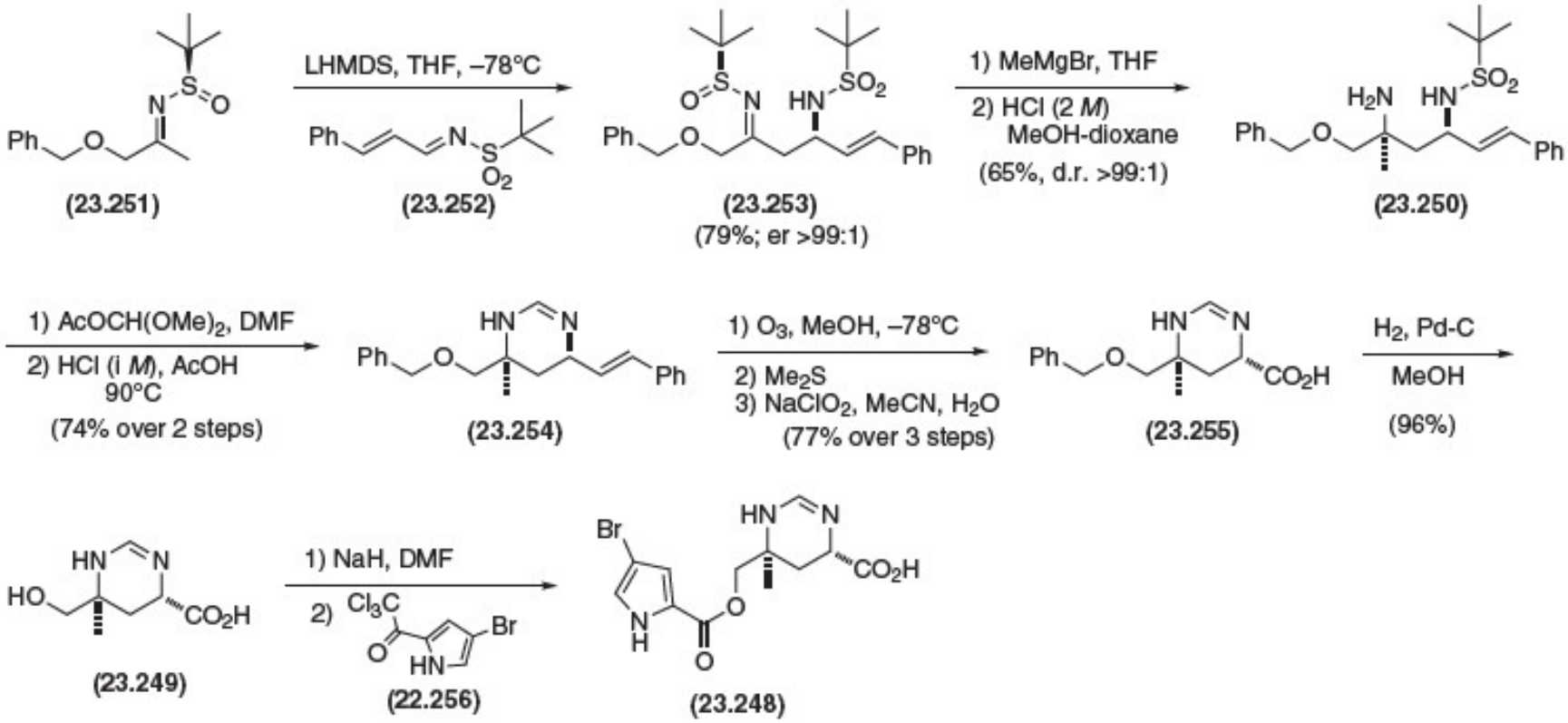

Synthesis of manzacidin-C by means of chiral control by a sulfinylamine chiral auxiliary

The enantioselective synthesis of ecklonialactones

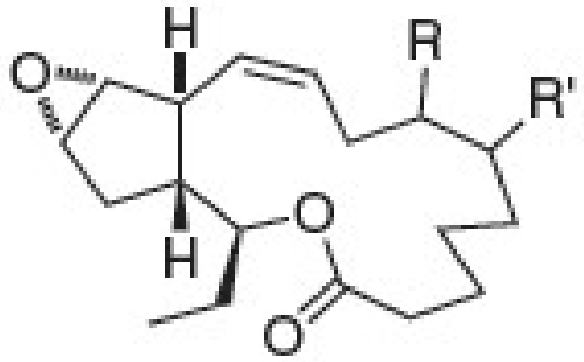

(23.257-A: R, R' = π bond)
(23.257-B: R = R' = H)

Figure 23.44

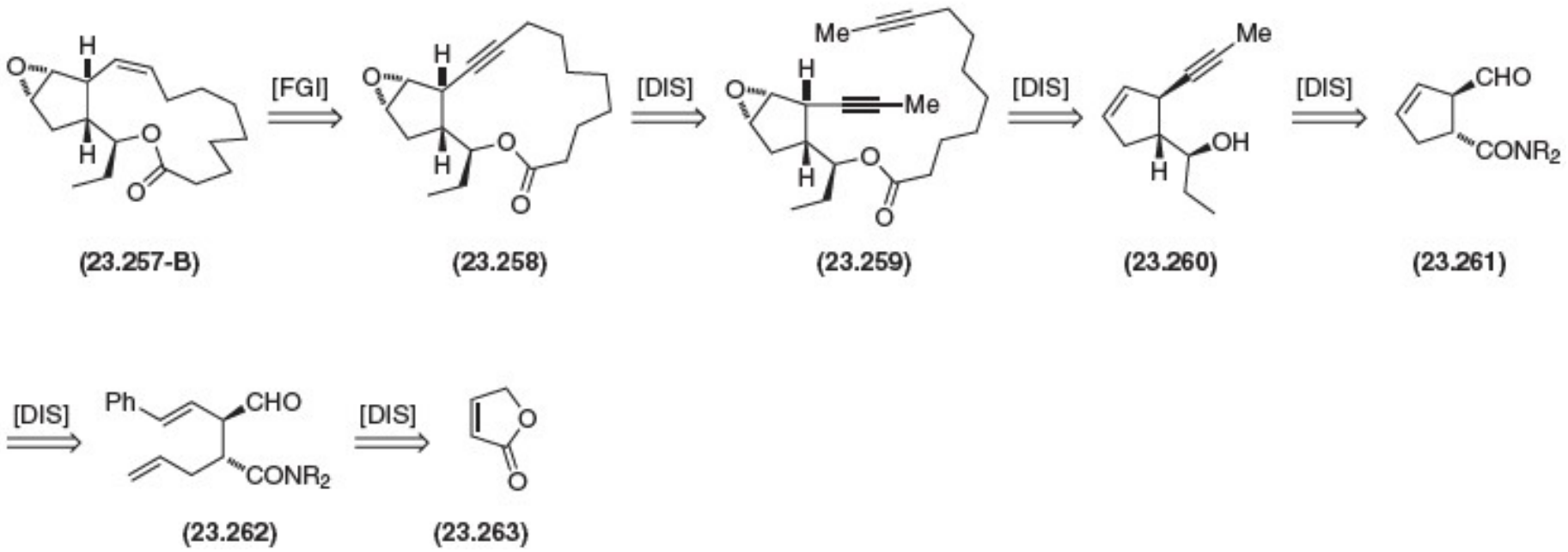

- Retrosynthetic analysis of ecklonialactone B

Figure 23.45

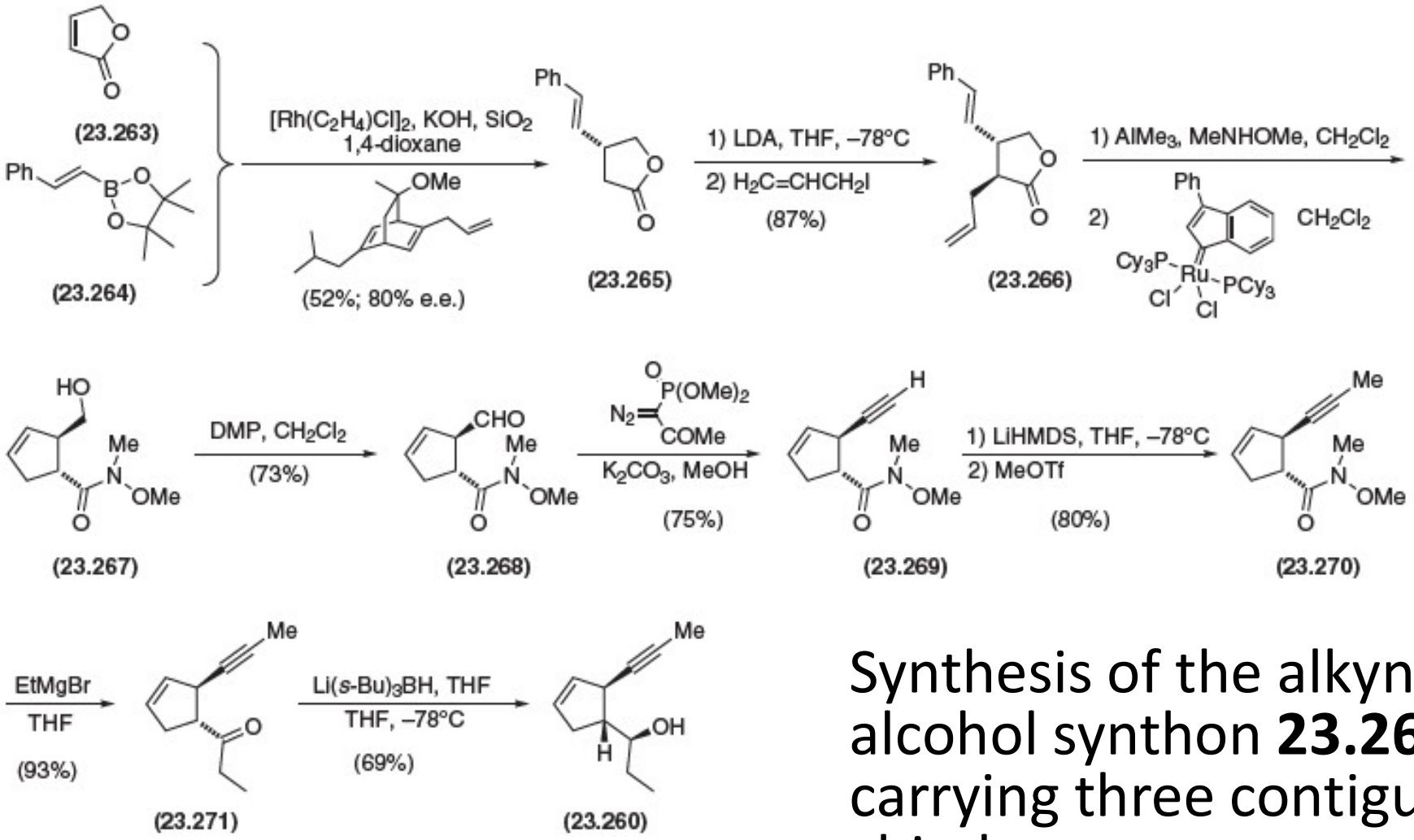

Synthesis of the alkynyl alcohol synthon **23.260**, carrying three contiguous chiral centers

Figure 23.46

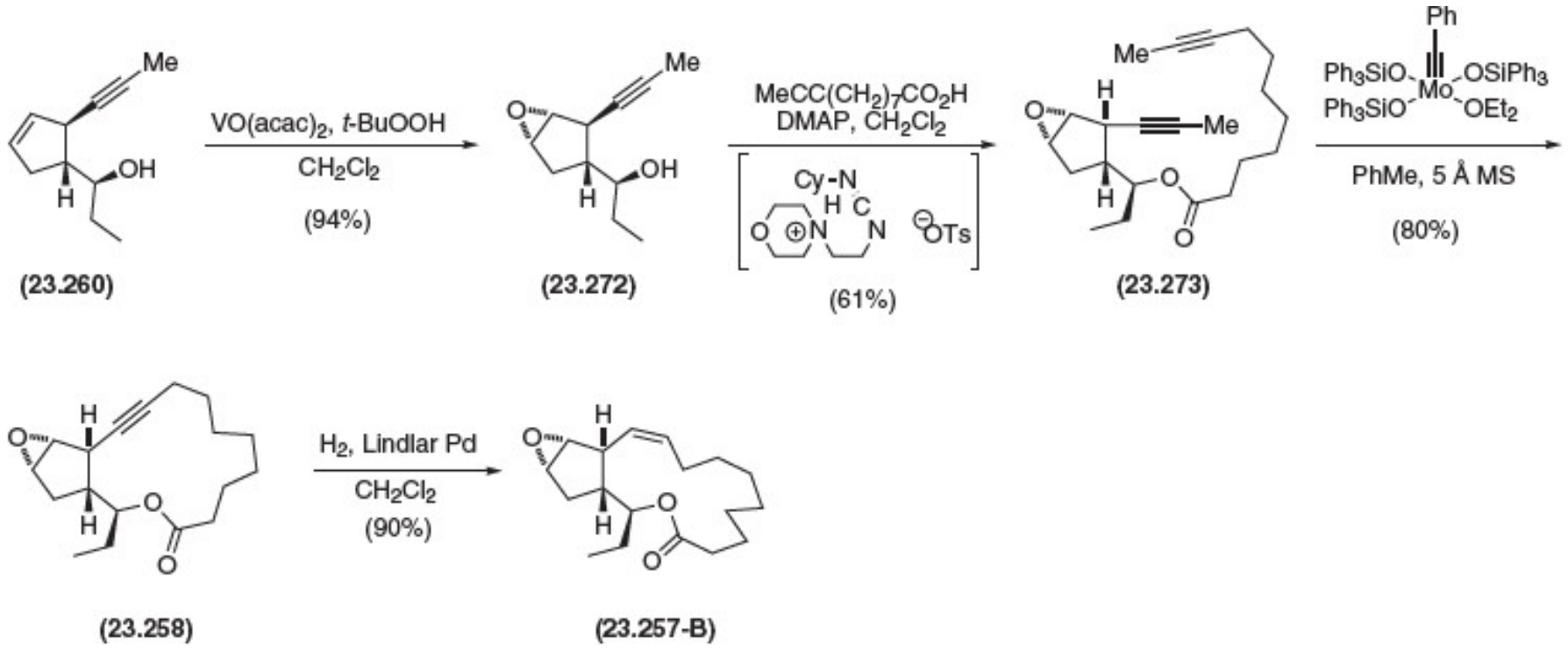

- Completing the synthesis of ecklonialactone B